

WITH SCIENCE



WE DEFEND

**TECHNICAL REPORT
NATICK/TR-99/020**

AD _____

DEMONSTRATION OF THE USE OF HYDROGEN FUEL FOR FOOD SERVICE

by
Dwight D. Back

**Mainstream Engineering Corporation
Rockledge, FL 32955**

March 1999

Final Report
October 1992 - September 1993

19990408 034

Approved for Public Release; Distribution Unlimited

Prepared for
**U.S. Army Soldier and Biological Chemical Command
Soldier Systems Center
Natick, Massachusetts 01760-5018**

DISCLAIMERS

The findings contained in this report are not to be construed as an official Department of the Army position unless so designated by other authorized documents.

Citation of trade names in this report does not constitute an official endorsement or approval of the use of such items.

DESTRUCTION NOTICE

For Classified Documents:

Follow the procedures in DoD 5200.22-M, Industrial Security Manual, Section II-19 or DoD 5200.1-R, Information Security Program Regulation, Chapter IX.

For Unclassified/Limited Distribution Documents:

Destroy by any method that prevents disclosure of contents or reconstruction of the document.

REPORT DOCUMENTATION PAGE

Form Approved
OMB No. 0704-0188

Public reporting burden for this collection of information is estimated to average 1 hour per response, including the time for reviewing instructions, searching existing data sources, gathering and maintaining the data needed, and completing and reviewing the collection of information. Send comments regarding this burden estimate or any other aspect of this collection of information, including suggestions for reducing this burden, to Washington Headquarters Services, Directorate for Information Operations and Reports, 1215 Jefferson Davis Highway, Suite 1204, Arlington, VA 22202-4302, and to the Office of Management and Budget, Paperwork Reduction Project (0704-0188), Washington, DC 20503.

1. AGENCY USE ONLY (Leave blank)	2. REPORT DATE March 1999	3. REPORT TYPE AND DATES COVERED FINAL Oct 1992 - Sept 1993
----------------------------------	------------------------------	--

4. TITLE AND SUBTITLE DEMONSTRATION OF THE USE OF HYDROGEN FUEL FOR FOOD SERVICE	5. FUNDING NUMBERS C DAAK60-93-C-0017
--	--

6. AUTHOR(S) Dwight D. Back	
--------------------------------	--

7. PERFORMING ORGANIZATION NAME(S) AND ADDRESS(ES) Mainstream Engineering Corp. 200 Yellow Place Rockledge, FL 32955	8. PERFORMING ORGANIZATION REPORT NUMBER
---	---

9. SPONSORING/MONITORING AGENCY NAME(S) AND ADDRESS(ES) U.S. Army Soldier and Biological Chemical Command Soldier Systems Center ATTN: AMSSB-RCF-E (N) Natick, MA 01760-5018	10. SPONSORING/MONITORING AGENCY REPORT NUMBER NATICK/TR-99/020
--	---

11. SUPPLEMENTARY NOTES

12a. DISTRIBUTION / AVAILABILITY STATEMENT Approved for Public Release; Distribution Unlimited	12b. DISTRIBUTION CODE
---	------------------------

13. ABSTRACT (Maximum 200 words) This Phase I effort demonstrated the use of hydrogen-gas fuel for use in food service applications. Energy efficiencies of 40-50 percent were achieved with Mainstream Engineering's hydrogen burner, with usable energy supply rates of 15,000 BTU/hr, fulfilling the requirements of the U.S. Army. It was demonstrated that hydrogen-fuel could be used for food service using compressed cylinders of hydrogen or by using metal-hydride derived hydrogen.
--

14. SUBJECT TERMS HYDROGEN FUEL ENERGY SOURCES RESEARCH AND DEVELOPMENT HYDROGEN BURNER EFFICIENCY HIGH ENERGY DENSITY FOOD SERVICE PROTOTYPE NON-POLLUTING	15. NUMBER OF PAGES 57
	16. PRICE CODE

17. SECURITY CLASSIFICATION OF REPORT UNCLASSIFIED	18. SECURITY CLASSIFICATION OF THIS PAGE UNCLASSIFIED	19. SECURITY CLASSIFICATION OF ABSTRACT UNCLASSIFIED	20. LIMITATION OF ABSTRACT SAR
--	---	--	---------------------------------------

Table of Contents

List of Figures	vii
List of Tables	viii
Preface	ix
1. Executive Summary	1
2. Section 1: Results of Phase I Effort	3
1.1 Introduction	3
1.2 Proof-of- Concept Burner System	5
1.3 Proof-of-Concept Burner Design Details	6
1.3.1 Hydrogen Nozzle	9
1.3.2 Burner Head	9
1.3.3 Air Entrainment Chamber	11
1.3.4 Mixing Chamber	11
1.3.5 Heat Transfer Limitations Between Flame and Kettle	12
1.4 Hydride Metal Selection	13
1.5 Operating and Test Conditions	16
1.6 Experiments and Experiment Results	16
1.6.1 Propane Experiments	18
1.6.2 Preliminary Hydrogen Experiments	18
1.6.3 Hydrogen Experiments	20
1.6.4 Hydrogen Verification Experiments	20
1.6.5 Metal-Hydride Burner Experiments	24
1.6.6 Additional Observations	24
Section 2: Summary of Phase 1 Tasks	26
Task 1 Literature Review	26
Task 2 Establish System Requirements	26
Task 3 Design of Hydrogen Fueled Kitchen	27
Task 4 Proof-of-Concept Experiments	27
Task 5 System Drawings and Reports	27

Table of Contents (Con't)

Section 3: Discussion of Results	28
Section 4: References	31
Appendix: Raw Data for Propane and Hydrogen Efficiency Studies	35

List of Figures

Figure	Page
1. Schematic of Hydrogen -Fueled Air-Entrainment Burner System	7
2. Detailed Drawing of Hydrogen-Air Burner	8
3. Flame Velocities as a Function of Fuel: Air Composition	10
4. Pressure-composition Isotherm for LaNi_5H_x at 25°C	15
5. Summary of Efficiencies Measured With M2 Burner: C_3H_8 and H_2	19
6. Effect of Energy Supply Rate (Hydrogen Flow Rate) on Burner Efficiency	21
7. Hydrogen Burner Efficiencies and Water Temperature	23
8a. The Use of Waste Burner Heat for Hydride Desorption	30
8b. The Use of Hydride Heat-of-Desorption for Refrigeration	30

List of Tables

Table	Page
1. Costs & Operating Conditions for H ₂ Kitchen: Operating at 50% Efficiency for 5 Hours	4
2. Physical and Chemical Properties Of LaNi ₅	14
3. Experiments for Propane-Fueled Studies	17
4. Experiments for Hydrogen Fuel Studies	17
5. Summary of Hydride Burner Experiments	25

Preface

This final report summarizes the Phase I effort performed by Mainstream Engineering Corporation on Contract DAAK60-93-C-0017, "Development of the Use of Hydrogen Fuel for Food Service". The research and development effort focused on the design of a hydrogen-fueled burner, and a demonstration of the hydrogen-fuel burner as an energy source in food service applications. The hydrogen used in the proof-of-concept demonstrations was supplied by either a compressed gas cylinder or metal hydrides.

The project was initiated by Muhammad Rahman, formerly with Mainstream Engineering, and completed by Dwight D. Back of Mainstream Engineering.

DEMONSTRATION OF THE USE OF HYDROGEN FUEL FOR FOOD SERVICE

EXECUTIVE SUMMARY

This Phase I effort successfully demonstrated the use of hydrogen-gas fuel for use in food service applications. Energy efficiencies of 40-50% were achieved with Mainstream's hydrogen burner, with *usable* energy supply rates of 15,000 BTU/hr, fulfilling the requirements of the Army. It was demonstrated that hydrogen-fuel could be used for food service using compressed cylinders of hydrogen or by using metal-hydride derived hydrogen. The use of metal hydrides to supply hydrogen would, however, require a more heat-transfer efficient design of the containment beds. An efficiently designed metal-hydride based system could also be used for refrigeration during the hydrogen-desorbing kitchen operation. For example, it is estimated that enough refrigeration energy (0.5-1.0 kW per burner) would be available to cool 178 gallons of water from 120°F to 70°F. Both hydrogen-supply systems are estimated to weigh less than 1,500 pounds for a 6-burner kitchen operating 3-5 hours, an approximate 18% weight increase for the entire Army kitchen trailer. The slight weight penalties associated with a hydrogen-fueled kitchen must be fully assessed alongside the favorable safety, efficiency, auxiliary cooling, and pollution-free factors.

The overall weight of the hydrogen burners would decrease as efficiencies are further improved. The heat transfer limitations of the current design could be improved for hydrogen use through optimization and redesign of the burner components by Mainstream's engineers. From the results of this effort, these design modifications could increase the overall efficiency above the 50% level. The crucial design factors identified in this Phase I effort, and the recommendations for enhanced burner-efficiency designs, would also be highly applicable to burners fueled by reactants other than hydrogen.

The use of hydrogen-fuel for food service is a viable application of the futuristic hydrogen-based technologies. Mainstream is strongly committed to integrating hydrogen fuel into the commercial and military energy economies since (1) hydrogen can be stored safely, (2) it is non-polluting with water being the primary combustion product, (3) hydrogen has a high energy density, (4) the fuel:air ratio is high relative to other fuels so that convective heat losses from nitrogen is minimized, and (5) hydrogen is a highly replenishable fuel.

This effort was initiated through a broad literature search to identify metal hydrides as hydrogen supply media and survey previous studies of hydrogen use in food service. Emphasis was placed on feasible field operations (weight, size, volume), also taking into account the safety, reliability, and ease-of-use of the storage technology. This search led to the purchase of LaNi₅ alloy from Ergenics, Incorporated. A burner design utilizing hydrogen fuel was also rendered taking into account safety issues pertaining to hydrogen volatility, combustion, and flame propagation velocities. The design was modeled after air aspirated devices such as the common Bunsen burner. Hydrogen nozzles were engineered to preclude flash-back of the combustion reaction to the hydrogen source, and a flash arrestor was also included to provide a second level of safety. The air entrainment and resulting hydrogen-air gas flow was designed to provide a high air:hydrogen ratio for complete hydrogen combustion (i.e., most efficient hydrogen usage) and flow rates

capable of stable flame velocities at the burner head. The current burner head used in the M2 burners was used throughout the design and testing of Mainstream's hydrogen-fueled burner.

Experiments were carried out with Mainstream's burner design using both propane and hydrogen fuel. Experiments were performed based on Taguchi experimental design methods, and verification experiments were performed to test the optimum parameter combinations determined from these experiments. Efficiencies were measured and compared to the 25% efficiencies typically obtained from gasoline-fueled M2 burners. The efficiency was determined by measuring the amount of hydrogen combustion energy utilized by 40 lb_m of water when heated from ambient to temperatures at, or near, boiling.

The results of these experimental efforts revealed that the efficiency of the burner is highly dependent upon the rate of heat supplied to the heated object (e.g., a kettle filled with water), the distance between the burner head/flame and the heated object, and the quantity of air aspirated into the hydrogen flow stream. The optimum settings for these factors were identified and found to be related to the limited heat transfer capability of the heated object. Further optimization improvements of the hydrogen-fueled burner would require the redesign of the burner head and heated-object geometry so as to (1) minimize convective and radiation heat losses between the burner head and heated object, (2) maximize the heat transfer area, (3) optimize the flame flow rate around the heated object to increase the heat-transfer-limiting gas-side heat transfer coefficient without overpowering the heat transfer capability of the burner/kettle system, and (4) maximize the hydrogen:air ratio to provide complete combustion of hydrogen. These issues and others would be rigorously addressed in a Phase II effort.

A successful Phase I effort demonstrated a safe, clean efficient, and dependable proof-of-principle burner prototype capable of utilizing hydrogen fuel. A Phase II effort would demonstrate working prototypes capable of food service over extended periods of time. The current national impetus to develop non-polluting fuels lends credence to hydrogen-fuel since the only by-product is water. Hydrogen is a high-energy density fuel, which can be stored and delivered from safe configurations. Aside from military field uses of a hydrogen-fueled burner, domestic kitchens and recreational food service are examples of commercial applications of the technology. Since hydrogen can also be used to generate electricity through fuel cells and hydride batteries, serve as a fuel for combustion engines, and provide refrigeration with the use of metal hydrides, a self-sufficient hydrogen fueled micro-city could be envisaged for the future. The use of hydrogen fuel for food service is a first step in this futuristic hydrogen-energy economy.

SECTION 1: RESULTS OF PHASE I EFFORT

1.1 Introduction

The Phase I effort, topic A92-074, "Demonstration of the Use of Hydrogen Fuel for Food Service", of DoD SBIR Solicitation 92.2 investigated the use of hydrogen as a fuel source in fuel service applications. Mainstream demonstrated a hydrogen-fueled, modified M2 burner capable of efficiencies between 40-50% (ratio of fuel energy utilized to fuel-value supplied). Modifications to the burner design were also addressed, which could further enhance this efficiency and reduce the overall weight of the 6-burner/5 hour kitchen. Heightened burner efficiencies would reduce cost, size, and weight of the hydrogen storage system used to supply the burner. The crucial design factors identified in this Phase I effort, and the recommendations for enhanced burner-efficiency designs, would also be highly applicable to burners fueled by reactants other than hydrogen.

The use of hydrogen as a fuel source provides a clean, safe and reliable approach to solve the world's energy demand (hydrogen is very abundant in water), providing an environmentally-conscience combustion process. The burner developed and demonstrated by Mainstream is a very crucial stepping-stone for a Phase II effort, and in realizing hydrogen-fuel technologies.

The current M2 burner utilizes a gasoline-air mix as fuel, with efficiencies of about 25%. The total usable energy demand required by the Army for these burners is about 15,000 BTU/hr, so that 60,000 BTU/hr of combustion energy must be supplied. As discussed in Progress Report #3 [27] for the Phase I effort, it was concluded that higher efficiencies might be attainable for hydrogen fuel due to higher fuel:air ratios required for combustion. Re-design of basic burner features will also lead to more efficient heat transfer. Mainstream has addressed both of these issues and can report much improved efficiencies between 40-50%, with a strong likelihood for further improvements since detailed burner re-design must still be addressed in a Phase II effort.

Table 1 summarizes a 6-unit hydrogen-fueled M2 burner kitchen operating at 50% efficiency for 5 hours. The system weight and size would decrease further as additional efficiency increases are developed. Note that the use of compressed hydrogen is competitive with the LaNi_5 hydride-supplied hydrogen on a cost and weight basis. For example, a hydrogen-cylinder supplied 6-burner system is estimated to weigh about 1,500 lb_m (50% efficiency), and if the burner efficiency is further increased to 75%, this weight would decrease to about 900 lb_m . As summarized in Table 1, the net increase in weight for a hydrogen-fueled system (relative to gasoline-fueled systems) operating at 50% efficiency would be approximately 1,000 lb_m , or a total kitchen trailer weight of about 6,635 lb_m . Additional weight savings could be achieved if higher weight per cent metal hydrides are used. For example, a 3 wt.% metal hydride operating at 75% efficiency would weigh about 400 lb_m including hardware, which is comparable to the 465 lb_m weight of the current gasoline fueled burner.

**TABLE 1 - COSTS & OPERATING CONDITIONS FOR H₂ KITCHEN:
OPERATING AT 50% EFFICIENCY FOR 5 HOURS**

hydride material cost	:	\$14,600/kitchen (initial cost)
hydrogen cost	:	\$25/lb _m H ₂ , or \$375/5 hr kitchen operation
hardware cost	:	estimate-25% of materials or \$3,640
hydride bed volume	:	6 x 1.2 ft ³
mass of hydride bed (s)	:	1,071 lb _m hydride + hardware @ 30% = 1,400 lb _m
metal-hydride capacity	:	1.4% hydrogen by weight
mass of burner hardware	:	20 lb _m (burner, flash arrestor, flow regulator)
operating temperature	:	ambient
burner efficiency	:	50%
hardware required	:	hydride tank, valve for flow control
TOTAL cost	:	\$18,240 (initial)+\$375/5 hr kitchen operation
TOTAL weight	:	approx. 1,400 lb_m with hardware
Fraction of TOTAL trailer weight	:	21%

OPTIONAL DESIGN WITH COMPRESSED GAS

mass of cylinder	:	125 lb _m /1.3 lb _m H ₂ or 1,440 lb _m for 6 burners
TOTAL cost	:	\$2,100 (initial hardware) + \$375/5 hr (H₂)
TOTAL weight	:	approx. 1,500 lb_m with hardware
Fraction of TOTAL trailer weight	:	23%

CURRENT M2 GASOLINE BURNER KITCHEN

TOTAL trailer weight	:	approx. 5,600 lb_m
TOTAL burner weight	:	360 lb_m (hardware) + 105 lb_m (fuel) = 465 lb_m
Fraction of TOTAL trailer weight	:	8.3%

The Phase I effort developed efficient burner designs and identified crucial design parameters for further increases in efficiency. The utilization of hydrogen-fuel was also a focal point of this effort. A summary of these efforts and the conclusions of the Phase I effort are given below:

- 1.) Hydrogen can be used as an efficient, non-polluting fuel source for food service applications;
- 2.) Burner efficiencies were measured in the range 40-50% with minor modifications to the current burner hardware and frame;
- 3.) The total weight for the hydrogen fuel source and burners for a 6-burner kitchen operating at 50% efficiency would be 1,500 lb_m or less, and the total kitchen trailer weight would be about 6,635 lb_m;
- 4.) Burner efficiencies might be enhanced further with redesign of the burner components, reducing the overall weight of the kitchen;
- 5.) Enhanced-efficiency burner designs would also be applicable to burners operating with fuels other than hydrogen;
- 6.) Hydrogen supplied by metal hydrides can be used as a hydrogen fuel source, but additional modifications to the hydride bed will be necessary for reliable operation;
- 7.) An efficient hydride-bed design could also provide refrigeration of 0.5 to 1 kW per burner;
- 8.) The use of compressed hydrogen as a fuel source is competitive with LaNi₅H₆ supplied hydrogen on a cost and weight basis. However, higher capacity hydrides would make compressed hydrogen less feasible.
- 9.) The gas-side heat transfer coefficient is the limiting resistance to heat transfer from flame to liquid.

1.2 Proof-of-Concept Burner System

A proof-of-concept burner was designed and fabricated using the burner head along with the supporting hardware of an Army M2 burner. A fuel-jet air-entrainment (FJAE) system was designed to replace the gasoline-air system of the current M2 burners.

The system was first studied with propane-air mixtures, and then with gas-cylinder hydrogen as a fuel. Since to achieve a 3 hour burn at 25% efficiency with a metal-hydride bed approximately 97 kg of alloy at \$39,000 would be required, the burner concept was first proven and refined using compressed hydrogen. Then, 1.5 kg of hydrided metal alloy was used to provide 1-3 minute burns at similar temperatures, pressures and flow rates as

used with the cylinder gas. Figure 1 is a schematic of the hydrogen-air burner system which can utilize both compressed hydrogen and hydride-generated hydrogen.

The delivered hydrogen gas (from the cylinder) was controlled by a pressure regulator and rotameter valve so that an upstream pressure of about 2 atm (30 psia) and flow rates of 0.25-1.0 lb_m H₂/hr were achieved. When using the metal hydride bed, no pressure regulation was used since the desorption pressure of the material is about 2 atm at 25°C. Mass flow rates in the range of 0.25-1.0 lb_m H₂/hr delivered to the burner at about 1 atm equate to energy supplies in the range of 15,200 to 61,000 BTU/hr, which covers the required energy supply (15,000 BTU/hr) after inefficiencies are taken into account. The hydrogen flow rates were determined by an analog pressure measurement and a calibrated flow meter (Omega Engineering model FL-3792ST). The hydrogen pressure delivered to the burner, downstream of the rotameter, was measured by an analog pressure gauge for use in mass flow rate calculations. A flash arrestor was placed between the hydrogen source and the FJAE as a safety precaution. The air intake rate to the FJAE will be adjusted by a sleeve designed to provide varying degrees of intake cross-sectional area and subsequent entrainment flow rates. A control lever and indicator was calibrated to control the shutter opening in 1/4 increments.

1.3 Proof-of-Concept Burner Design Details

Figure 2 is a detailed drawing of the hydrogen-air burner system. The material of construction for the burner nozzle, entrainment section, mixing section and spacers was aluminum. Aluminum was selected for its weight and ease of machining. Since the burner was designed so that a stable flame at a temperature of about 2000°C would only be present at the burner head, a temperature approaching 660°C (melting point of aluminum) was not anticipated in the lower sections of the burner assembly. The burner sections were machined to close tolerances so the individual pieces were connected by snug press fits. A Matheson Flash Arrestor, model 6103, was used to preclude flame flashback to the hydrogen supply, and an Omega rotameter, model FL-3792ST, was used for flow rate measurements. After regulating the supply hydrogen to a desired upstream pressure, the burner was operated by opening the hydrogen gas supply valve on the rotameter to achieve the desired experimental flow rate. The air entrainment shutters were then set to the closed position, and a lighter was used to ignite the hydrogen:air mixture flowing from the burner head. The air entrainment shutters, graduated in 1/4, 1/2, 3/4, FULL positions, were then adjusted to the desired experimental setting. To reduce the distance between the burner head and kettle bottom from 5" (as in some experiments), spacers were added between the fuel mixing section and the burner head. The spacers provided a varying distance between burner head and kettle, with a minimum value of 1".

The burner system was designed to supply hydrogen:air mixtures to the burner head in the air-rich regime of combustion. Fuel rich mixtures and subsequent incomplete combustion of hydrogen would result in lower burner efficiencies. The velocity of the hydrogen flowing from the nozzle was also designed to exceed the reported flame velocities of hydrogen:air flames (to avoid flashback through the nozzle), and the velocities of the

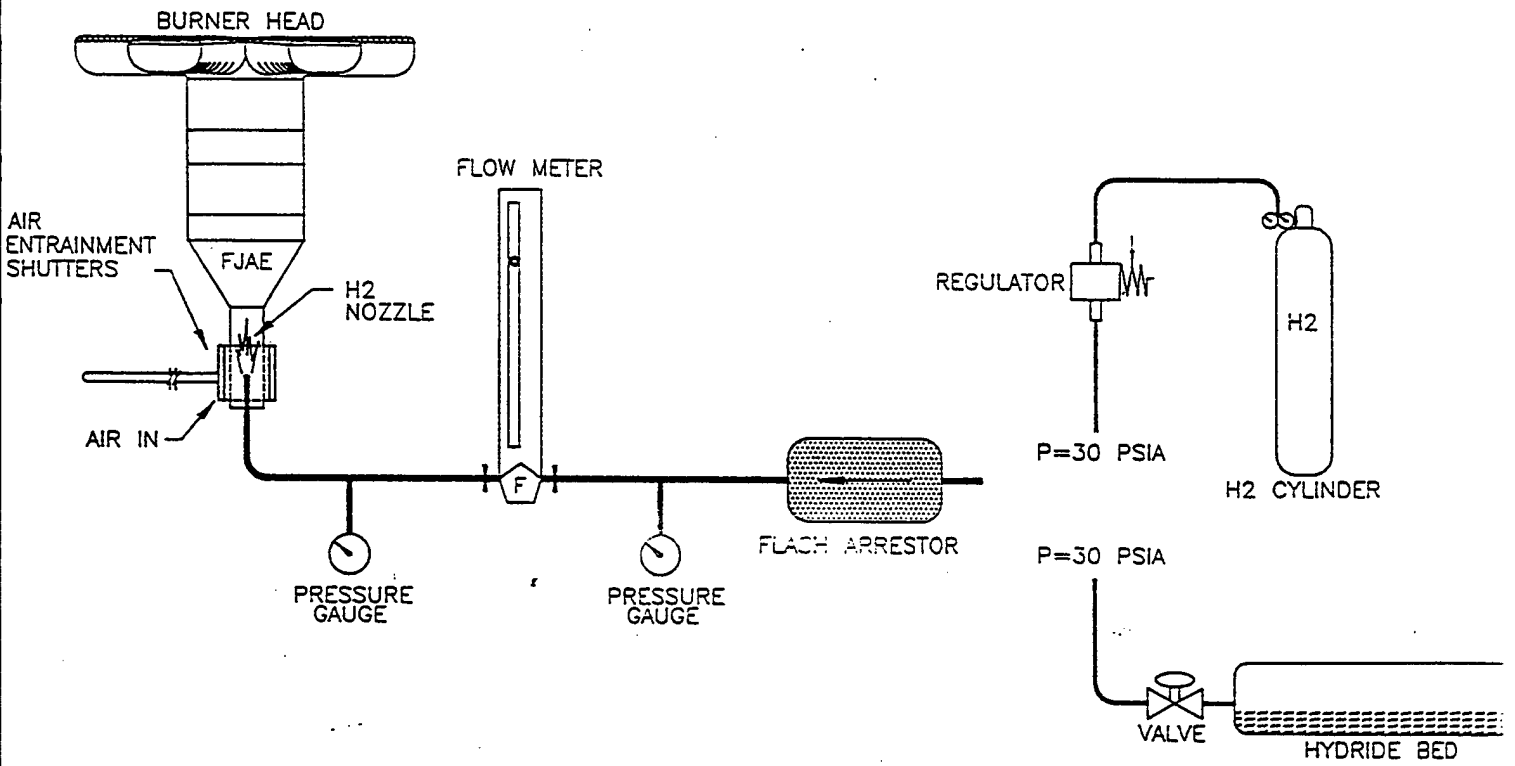


Fig 1. Schematic of Hydrogen-Fueled Air-Entrainment Burner System

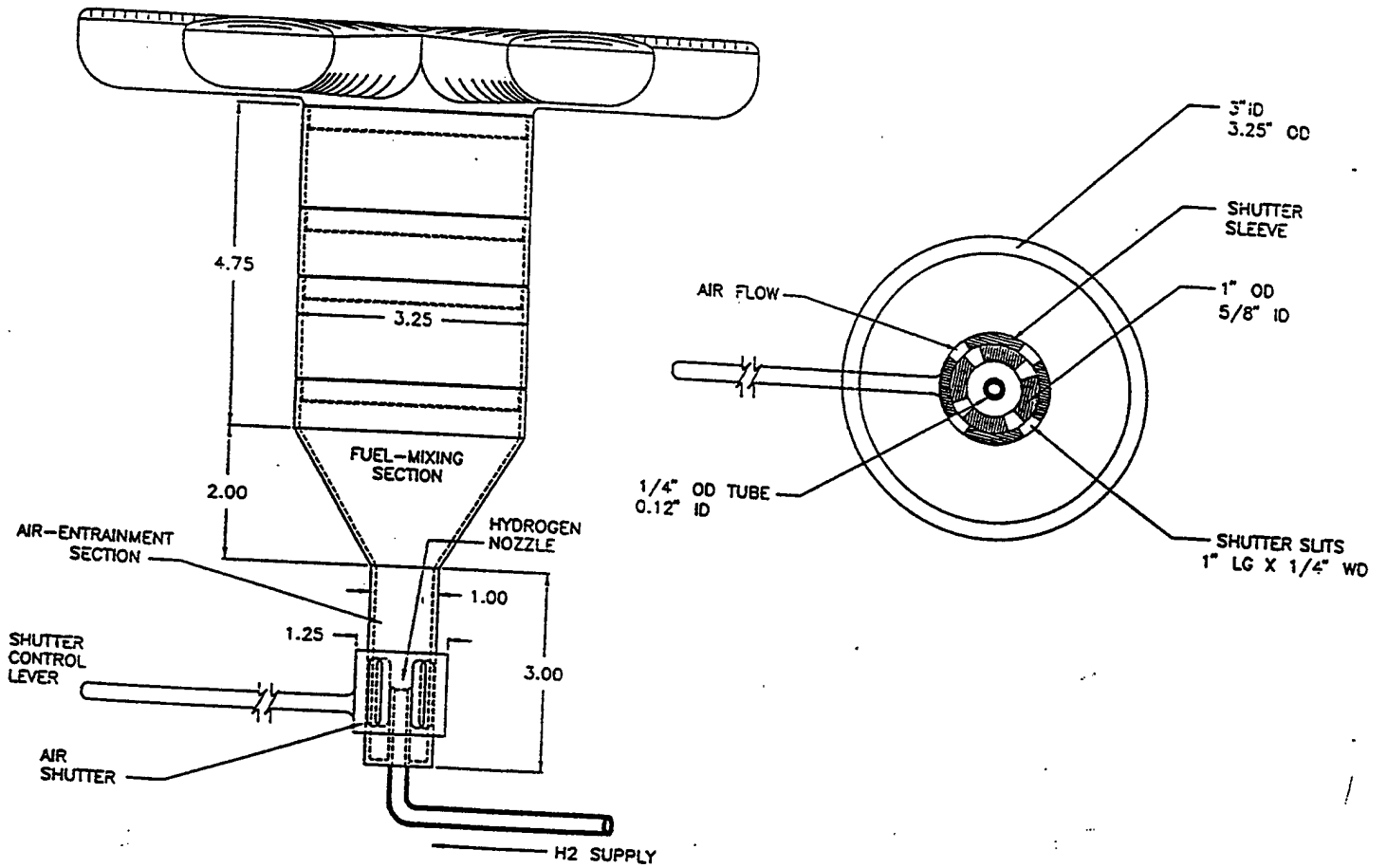


Fig 2. Detailed Drawing of Hydrogen-Air Burner

hydrogen:air mixture through the burner opening was also designed for a flow range in which stationary flame velocities can be achieved.

The following is a detailed discussion of the components of the burner system. The calculations presented are meant as examples of engineering estimates used to design the proof-of-concept hydrogen burner hardware. The numerical figures should not be construed as strict design criteria.

1.3.1 Hydrogen Nozzle: The hydrogen nozzle located in the FJAE has been designed such that the exit velocity would be greater than the maximum flame velocity of 10 ft/s (~325 cm/s) of air/hydrogen mixtures and less than the acoustic velocity of hydrogen at 300°K (1.3×10^5 cm/s). For some experiments, a screen was also placed below the burner head in the FJAE in order to increase the degree of air/hydrogen mixing. Accordingly, the inside diameter of the nozzle was sized to 0.12" yielding a velocity of 344 ft/s (1.0×10^4 cm/s) hydrogen at 15 psia, 0.5 lb_m H₂/hr, and 25°C. For flow rates of 0.25 lb_m H₂/hr, the exit velocity was approximately 172 ft/s, still a factor of 17 larger than the maximum flame velocity of 10 ft/s, thus precluding flashback hazards. A typical Reynolds number for the hydrogen flow from the nozzle is $Re = D\rho\langle v \rangle / \mu = (0.12 \text{ in}) \times (2.54 \text{ cm/in}) \times (1.62 \times 10^{-4} \text{ g/cm}^3) \times (344 \text{ ft/s}) \times (30.48 \text{ cm/ft}) / (187.5 \times 10^{-6} \text{ g/cm-s}) = 2,763$.

1.3.2 Burner Head: The existing M2 burner head was used throughout the experiments with only minor modifications: The central hole, located on the top of the head, used in the standard gasoline burner was plugged so that all of the fuel mixture would flow through the slits. The remaining design considerations for the burner head focused on delivering an appropriate exiting flame velocity capable of sustaining a stable flame over a range of hydrogen:air ratios.

It might be assumed as a first approximation that the gas mixture velocity through the burner head slits will be 110 cm/s (3.6 ft/s) at stoichiometric proportions of hydrogen/air (see Figure 3). A more rigorous estimate is arrived at from the hydrogen flow rate, assuming an entrainment flow of the air, and then calculating the flow velocity from this volumetric flow rate and the exiting burner head cross section area. For example, consider a hydrogen flow rate of 0.027 ft³/s or 0.25 lb_{mol} H₂/hr (0.5 lb_m H₂/hr) at 15 psia and 25° C. Assuming a stoichiometric mix of 2 mole H₂/mole O₂ (i.e., the stoichiometric requirement of air is entrained through the air shutters), then $(0.25 \text{ lb}_{\text{mol}} \text{ H}_2) \times (1 \text{ mole O}_2 / 2 \text{ mole H}_2) \times (1 \text{ mole air} / 0.21 \text{ mole O}_2) = 0.6 \text{ lb}_{\text{mol}} / \text{hr}$ air is entrained/mixed. The total hydrogen-air mixture at approximately 1 atmosphere pressure is then $0.6 + 0.25 = 0.85 \text{ lb}_{\text{mol}} / \text{hr}$ gas mix, which equates to about $(0.85 \text{ lb}_{\text{mol}} / \text{hr}) \times (10.73 \text{ ft}^3 \text{ psia} / \text{lb}_{\text{mol}} \text{ } ^\circ\text{R}) \times (530^\circ \text{ R}) / (14.7 \text{ psia}) = 329 \text{ ft}^3 / \text{hr}$ or 0.091 ft³/s for an ideal gas.

The 109 burner slits of the M2 burner each have an approximate cross sectional area of 0.0469 in² or 3.25×10^{-4} ft². Using the above figure of 0.091 ft³/s for volumetric flow rate, the flow rate through each slit will be approximately $0.091 \text{ ft}^3 / \text{s} \div 109 = 8.35 \times 10^{-4} \text{ ft}^3 / \text{s}$, so that the velocity through each slit will be $(8.35 \times 10^{-4} \text{ ft}^3 / \text{s}) \div (3.25 \times 10^{-4} \text{ ft}^2) = 2.6 \text{ ft/s}$. Referring to Figure 3, the hydrogen-air composition for a flame velocity of 2.6 ft/s is

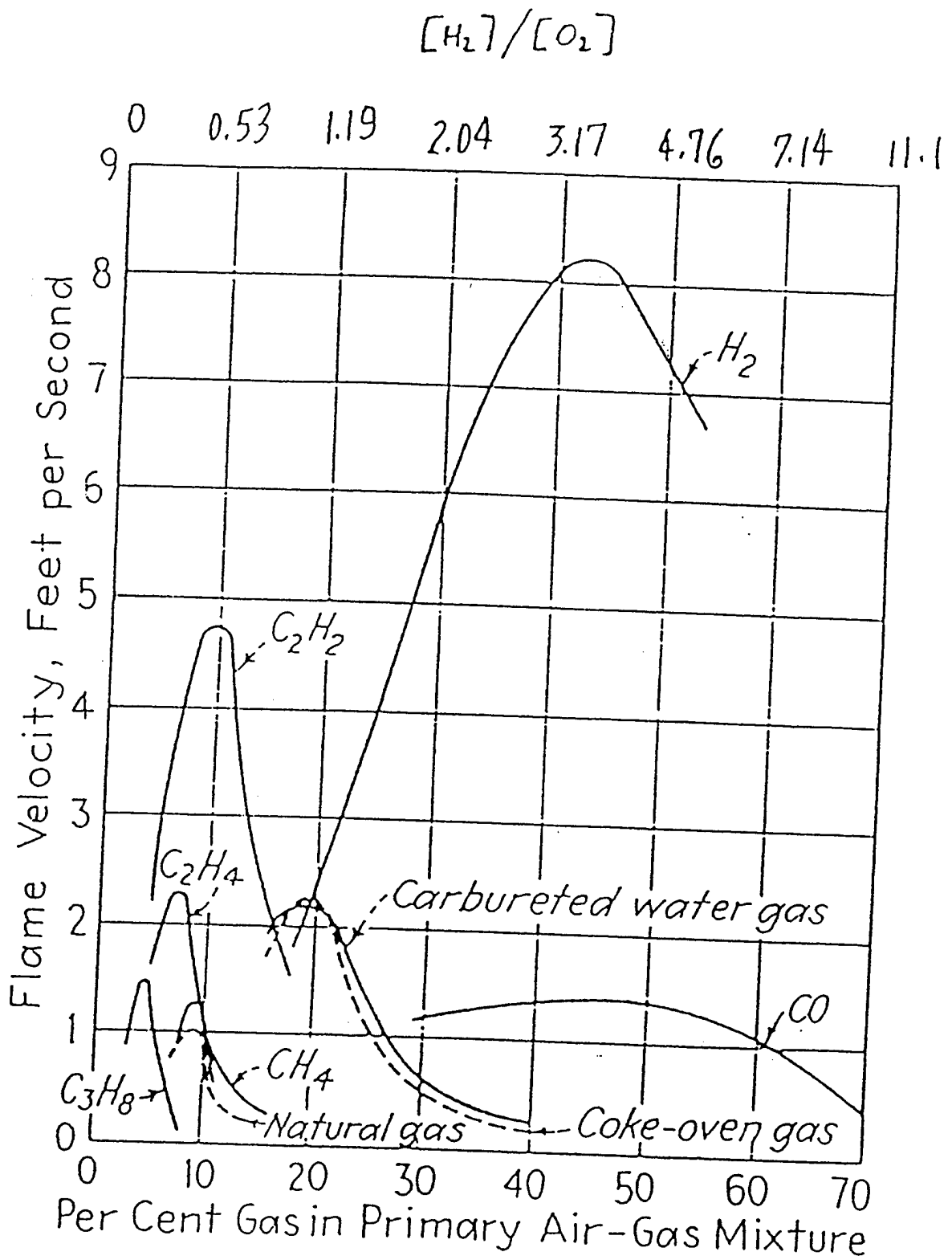


Figure 3. Flame Velocities as a Function of Fuel:Air Composition [reference 29]

roughly 25%, which is very close to the velocity for the assumed stoichiometric proportion above (2 mole H₂/mol O₂ or 30% hydrogen in air). In order to increase the flame velocity exiting the burner head slits, stainless sleeves were fabricated which slipped over each of the 6 burner head fingers. The effective reduction in cross sectional area of the burner-exit area increased the exiting flame velocity proportionally. These area-reduction sleeves were only used for preliminary propane and hydrogen experiments, since it was determined that flow through the blocked slits and around the sleeves was still occurring.

1.3.3 Air Entrainment Chamber: The air entrainment section of the burner provides for a supply of air from ambient as a result of the pressure gradient generated by the fast-flowing hydrogen fuel. This 'venturi' effect can then be controlled by opening the air shutters to varying degrees to provide fuel-rich and air-rich mixtures of gas supplied to the burner head.

A rough approximation will serve to illustrate the entrainment process. Consider a hydrogen stream flowing from the fuel nozzle at a velocity of 344 ft/s (15 psia, 0.5 lb_m H₂/hr). Since the air near the wall of the entrainment section will have a velocity of zero ('no slip' boundary condition) and the velocity at the thin fuel jet near the center of the entrainment section will be roughly 344 ft/s, the average velocity of the entrained air will be approximately the average of these values, or 344÷2=172 ft/s. Since the total cross sectional area of the 4 air entrainment shutters (fully opened) is 4x(1"x0.25")=1 in² or 6.94x10⁻³ ft², the estimated flow rate is (6.94x10⁻³ ft²)x(172 ft/s)=1.2 ft³/s at 1 atm, or about (1.2 ft³/s)x(14.7 psia)/(10.73 ft³ psia/lb_{mol} °R)x(530°R)=3.1x10⁻³ lb_{mol} air/s = 11.2 lb_{mol} air/hr. Since the hydrogen molar flow rate under these specified conditions is 0.25 lb_{mol}/hr, the hydrogen:air mixture would be 0.25:5.8 or about 2%. This composition represents a highly air-rich mixture, and fuel enrichment can subsequently be achieved through closure of the air shutter. For example, some experiments were run with the shutter at 1/4 open: the effective shutter cross sectional flow area would then be 0.25 in², which equates to about 2.8 lb_{mol} air/hr, or 9% hydrogen in air. At the fully shut position of the air shutter, air is still entrained to a limited degree due to the tolerances between the fittings of the burner. Thus, a completely fuel-rich gas stream can not be achieved in practice, and it should be noted that such an operating condition is not desirable --- complete and efficient combustion of the hydrogen will only be achieved with hydrogen:air mixtures having a composition of 30% (vol.) hydrogen or less.

1.3.4 Mixing Chamber: The mixing section of the burner was designed to provide for fuel:air mixing before entering the burner head section of the burner. A rough approximation of the mixing length required to achieve the mixing of two gas streams is obtained from [28]. The mixing of a fluid jet into a relatively stagnant fluid is described by the equation:

$$\frac{q_e}{q_o} = \left(\frac{X}{4.3D_j} - 1 \right) \quad [\text{Eq. 1}]$$

where q_e is the volume of fluid entrained per unit time at a distance X from the nozzle, q_0 is the volumetric flow rate of fluid leaving nozzle, and D_j is the diameter of the nozzle. Assuming that a stoichiometric mixture of hydrogen:air is required to be mixed, then q_e/q_0 will be approximately equal to 70 mol air/30 mol H_2 (see Figure 3, or reference 29), or X/D_j must be greater than or equal to 14.3. Since the nozzle diameter is 0.12", the length of the mixing and entrainment section must be at least 1.75" (0.12"x14.3). The burner was designed to exceed this length with a 3" entrainment section *plus* a 2" mixing section = 5". Additional spacer sections also provide an additional 4.75" of mixing length (see Figure 2) --- these spacers were used to adjust the distance between the bottom of the kettle and the burner head. Note also that in addition to entrainment, mixing occurs as a result of the high shear stresses present at the boundary between the jet and stagnant fluid, producing localized vortices which also enhance mixing. A screen having a mesh size of 100 was also inserted in this section to create turbulence and induce further mixing. It is believed that the designed studied in this effort would produce sufficient mixing so that the hydrogen:air gas mixture exiting the burner head was well-mixed prior to combustion.

1.3.5 Heat Transfer Limitations Between Flame and Kettle: Due to possible limitations in heat transfer processes between the flame, having a temperature of about 2000°C [30], and the kettle, some inefficiencies could result if the energy supplied by the combustion mixture exceeds the capability of the kettle in absorbing the energy. Consequently, a brief analysis is necessary to evaluate the order of magnitude heat transfer rates with a 2000°C flame and water at about 100°C. The heat transfer resistances which must be considered are (1) forced-convective heat transfer between the flame and kettle, (2) conductive heat transfer through the stainless steel kettle, and (3) free-convective heat transfer between the kettle and the liquid in the kettle (i.e., water or boiling water). The overall heat transfer coefficient can be estimated from the expression:

$$U = \frac{1}{\frac{1}{h_{liq}} + \frac{\Delta x}{k} + \frac{1}{h_{gas}}} \quad [\text{Eq. 2}]$$

and the heat transfer rate would be given by

$$q = AU\Delta T = AU(T_{flame} - T_{water}) \quad [\text{Eq. 3}]$$

For use in the above equations, assume the following: a kettle wall thickness of 1/8", a kettle diameter of 17" (cross sectional area of 1.6 ft²), ΔT of (2000°C-100°C)=1900°C (3420°F), thermal conductivity k for stainless steel of 24 BTU/ft-hr°F, a gas-side heat transfer coefficient equal to 10 BTU/ft²hr°F [reference 31: average value for forced-convection heat transfer coefficient], and a liquid-side heat transfer coefficient equal to 2000 BTU/ft²hr°F [35: average value for boiling water]. The *estimated* heat transfer rate using these values results in

$$q = 1.6 \text{ ft}^2 \times \frac{1}{\frac{1}{2000} + \frac{0.01}{24} + \frac{1}{10}} \times 3420^\circ \text{ F} = (1.6 \text{ ft}^2)(9.9 \text{ BTU} / \text{ft}^2 \text{ hr}^\circ \text{ F})(3420^\circ \text{ F}) = 54,200 \text{ BTU} / \text{hr}$$

[Eq. 4]

The limiting resistance to heat transfer in this analysis is due to the gas-side heat transfer, and the value arrived at above is of similar order to the approximate 60,000 BTU/hr supplied to the current M2 burner. Although the above figure should be viewed only as an estimate, it does indicate that operation of the M2 burner at heat supply rates approaching 60,000 BTU/hr could be at or near the heat transfer capability when heat losses from the kettle to ambient (radiation and convective) are included (i.e., reducing the limiting heat transfer value q even further). The implications of heat transfer limitations could also become more of an issue if the flame, at a temperature of 2000°C, is not efficiently contacting the bottom of the kettle, thereby decreasing the temperature differential ΔT . Consequently, for efficient design of the burner the following factors must be carefully selected and optimized: (1) distance between burner head and kettle, (2) convective and radiation heat losses from the hot kettle to ambient, (3) heat supply rate of the combustible fuel, (4) surface area of the kettle, and (5) fluid flow properties such as the Reynolds number of the combustion flame along the bottom of the kettle (i.e., the heat transfer rate for the gas is strongly dependent on this Reynolds number).

1.4 Hydride Material Selection

A LaNi_5 alloy was chosen as the hydride material. This material has favorable pressure-composition behavior at ambient temperatures, can be activated at moderate temperatures and pressures, is readily available commercially, and has been studied considerably in the past. Table 2 describes the physical/thermodynamic properties of the LaNi_5 alloy, and Figure 4 is a pressure-composition isotherm for the materials at 25°C. Reference [32] provides a thorough review of metal hydrides and their properties.

In general, metal hydrides can be poisoned by O, C, N, H_2O , Cl, Na, and several other impurities. Nitrogen is typically not a problem with LaNi_5 , and O and H_2O can be removed by vacuum heating. Other ions such as Cl can poison the surface and also reduce the capacity of the material.

For a 3 minute burn of hydrogen, it was estimated that about 1.5 kg (3.3 lb_m) of LaNi_5 is required. Consequently, a 1 liter cylinder was loaded with LaNi_5 and charged with hydrogen after activation. The activation process was accomplished by first heating the alloy under vacuum (less than 50 mTorr or 0.001 psia) at about 150°C, cooling to room temperature, and then loading with hydrogen. Some difficulties were encountered during the activation process, and it was suspected that the vacuum system was contaminated with chloride and other salts, water, and high molecular-weight organic compounds from past projects. To initiate and accelerate the hydrogen activation process a pressure of 500 psig H_2 was used. Approximately 10 charges of 500 psig H_2 were required to fully load

TABLE 2 - PHYSICAL AND CHEMICAL PROPERTIES OF LaNi₅

Molecular weight = 432.5 g/mol

Metallic density = 8.4 g/cm³

Apparent density of powder (after activation) \approx 4.5 g/cm³

Dissociation pressure at \sim 25°C = 1.7-2.0 atm (24-30 psia)

Hydrogen desorption rate at 25°C & 2 atm: approx. 34.9 (liter H₂/min)/kg LaNi₅

Volume expansion, LaNi₅ \Rightarrow LaNi₅H₆ \approx 25%

Weight % H at full capacity = 1.4%

$\Delta H_f = 7.4$ kcal/mol H₂ (6,667 BTU/lb_m H₂)

$k = 3.15 \times 10^{-4}$ kcal/m-s-°K (0.762 BTU/ft-hr-°F)

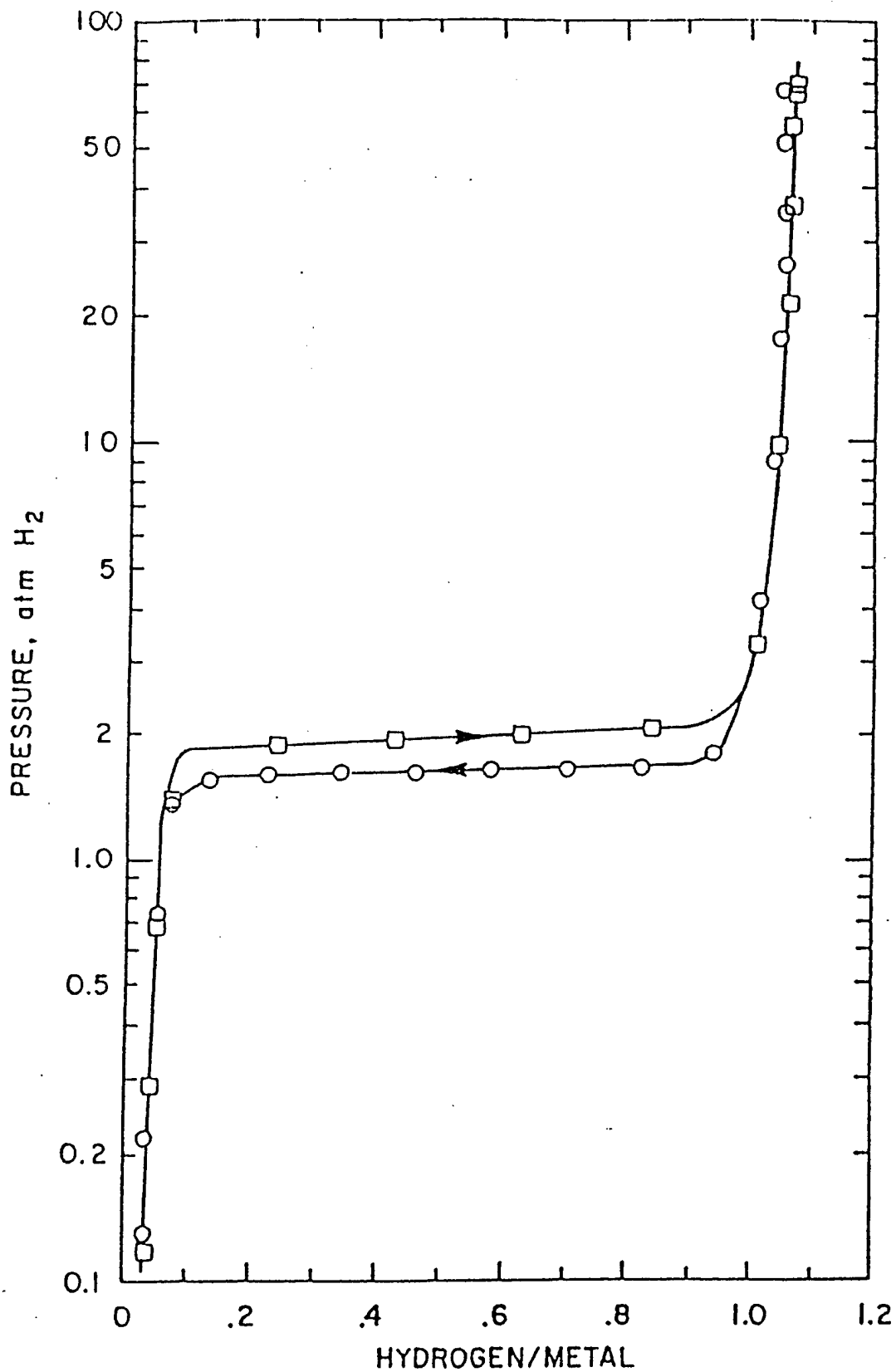


Figure 4. Pressure-composition Isotherm for LaNi₅H_x at 25°C [reference 32]

the LaNi_5 alloy to LaNi_5H_6 . For future activation processes, it is highly recommend to use a dedicated vacuum system.

The heat-of-reaction (ΔH_r) for the hydrogen desorption process is endothermic requiring about $6,667 \text{ BTU/lb}_m \text{ H}_2$ of heat. It was found during the course of this effort that natural convection of air around the hydride cylinder was insufficient to supply the required endothermic heat during desorption. Consequently, this heat transfer limitation prevented a sustained 3-minute supply of hydrogen at the flow rates used in the compressed hydrogen efficiency studies. A summary of several hydride burner experiments is given in Table 5 of section 1.6. To maintain the temperature of the hydride bed at or above ambient temperature, heat was supplied by heat tape or heated water. Future hydride bed designs will probably require extended surface area, the use of waste heat from the burner, and possibly a heat transfer media other than air (e.g., water). The endothermic desorption reaction, providing up to $(6,667 \text{ BTU/lb}_m \text{ H}_2) \times (0.5 \text{ lb}_m \text{ H}_2/\text{hr}) \times (1 \text{ W}/3.41 \text{ BTU/hr}) = 980 \text{ W}$ of cooling, which could be used as a field refrigeration source.

1.5 Operating and Test Conditions

To study the efficiency of the hydrogen-fueled M2 burner, experiments were devised with both hydrogen and propane. The variables considered in the experiments were fuel-supply flow rate, air-shutter opening, burner head flow cross-sectional area (C_3H_8 only), and burner head height (distance from burner head to bottom of kettle). As discussed in section 1.3, these variables will effect efficiencies through variations in convective heat losses, energy supply rates, and fuel:air mixture composition.

Two partial factorial experiments utilizing Taguchi Design of Experiments techniques [33] were used to study the effects of these variables on burner efficiency. The following experiments were carried out: 1 experimental set with propane as a fuel, 1 preliminary experiment with hydrogen using the same setup as the propane experiments, 1 experimental set with hydrogen as the fuel and an improved burner design, and 4 verification experiments with hydrogen to study the optimum design. The verification studies were performed to test the effects of the hydrogen supply flow rate and air shutter opening in more detail. The details of these efforts are discussed in section 1.6. The experiments and the conditions are summarized in Tables 3 and 4.

1.6 Experiments and Experimental Results

As described in Tables 3 and 4, propane and hydrogen fuels were evaluated on a basis of efficiency, defined as the per cent of fuel used to heat 40 lb_m of water over a temperature range up to the boiling point of water, 212°F (100°C). The fuel-energy supplied is calculated from the pressure of the fuel P_{fuel} supplied to the burner and the measured flow rate \dot{V} of the gas prior to entering the nozzle of the burner chamber (see Figures 1 and 2):

TABLE 3 - EXPERIMENTS FOR PROPANE-FUEL STUDIES

RUN	A.) Air S	B.) Brn H	C.) Flw R	Effect
1	1	1	1	12.1
2	1	2	2	14.1
3	2	1	2	8.6
4	2	2	1	11.0
level 1	13.1	10.4	11.6	Grand Avg.
level 2	9.8	12.6	11.4	11.5
total effect	3.3*	2.2	0.2	

- Air S=AIR SHUTTER POSITION: 1=1/4 open, 2=3/4 open
- Brn H=BURNER HEAD SLIT OPENING: 1=1/2 open, 2=fully open
- Flw R=GAS SUPPLY FLOW RATE: 1=5 scfh air, 2=20 scfh air
- Distance from burner head to kettle bottom=constant=5", gas supply pressure=20 psig

TABLE 4 - EXPERIMENTS FOR HYDROGEN-FUEL STUDIES

RUN	A.) Air S	B.) Brn H	C.) Flw R	Effect
1	1	1	1	35.5
2	1	2	2	23.0
3	2	1	2	18.0
4	2	2	1	21.2
level 1	29.3	26.8	28.4	Grand Avg.
level 2	19.6	22.1	20.5	24.4
total effect	9.7*	4.7	7.9	

- Air S=AIR SHUTTER POSITION: 1=1/4 open, 2=FULL open, 3=CLOSED
- Brn H=DISTANCE BETWEEN BURNER HEAD AND KETTLE BOTTOM: 1=1" from kettle bottom, 2=2.5" from kettle bottom
- Flw R=GAS SUPPLY FLOW RATE (N064-63ST): 1=rotameter@10, 2=rotameter@20, 3=rotameter@5

$$E(\text{supplied}) = E^* \cdot (MW) \cdot \left(\frac{P_{\text{fuel}} \dot{V}}{RT} \right) \cdot \Delta t \quad (\text{BTU}) \quad [\text{Eq. 5}]$$

where E^* is the energy value of the fuel: (61,000 BTU/lb_m H₂ and 19,900 BTU/lb_m propane), MW is the molecular weight of the fuel, R is the ideal gas constant, T is the ambient temperature, and Δt is the time between water temperature readings. The fuel and energy utilized in heating the 40 lb_m of water is calculated by

$$E(\text{utilized}) = m_{\text{water}} \cdot C_p \cdot \Delta T_w \quad (\text{BTU}) \quad [\text{Eq. 6}]$$

where C_p is the heat capacity of water (approx. 1.0 BTU/lb_m°F), m_{water} is the mass of water, and ΔT is the temperature change of the water. The efficiency of the burner is then evaluated between each water-temperature measurement as a function of time, and the overall or "lump" efficiency of the burner is calculated from the time t_{final} it takes to heat the water from its initial temperature T_{initial} to the final temperature T_{final} , which in most cases was the boiling point:

$$\eta_{\text{lump}} = \frac{m_{\text{water}} \cdot C_p \cdot (T_{\text{final}} - T_{\text{initial}})}{E^* \cdot (MW) \cdot \left(\frac{P_{\text{fuel}} \dot{V}}{RT} \right) \cdot t_{\text{final}}} \times 100\% \quad [\text{Eq. 7}]$$

Typically, the experiments lasted 20 minutes to 1 hour. A summary of efficiencies measured in this effort for hydrogen and propane are shown in Figure 5. In general, the burner efficiencies measured with the original M2 burner configuration (approx. 5" between the burner head and kettle) were considerably lower than those measured for hydrogen with a 1" distance between the components. This effect is illustrated by comparing the 'propane' and 'preliminary hydrogen' experiments with the 'verification hydrogen' experiments. The details of these experiments are described below.

1.6.1 Propane Experiments: Table 3 shows the results of initial experiments with propane as a fuel, and Appendix C shows the detailed evaluation data of all experiments. The column labeled "effect" in Table 3 is the calculated η_{lump} . The average efficiency for the propane experiments was 11.5%, and using the methods of Taguchi the variable with the greatest effect was the air shutter opening (denoted by and '*' in the table). That is, the supply of air had the greatest influence on the efficiency of the burner. The 'effect' is the last row in the data tables of Tables 3 and 4, and is essentially the range of efficiency values produced by changing the variable between 'level 1' and 'level 2'. These experiments made use of the FJAE burner design and a distance of 5" between the burner head and kettle bottom (current M2 burner configuration).

1.6.2 Preliminary Hydrogen Experiments: After noting the low burner efficiencies with propane, a single experiment with hydrogen was performed adhering to the parametric conditions of experiment #3 of the propane experimental matrix. The resulting efficiency

Burner Efficiencies for Hydrogen and Propane Experiments

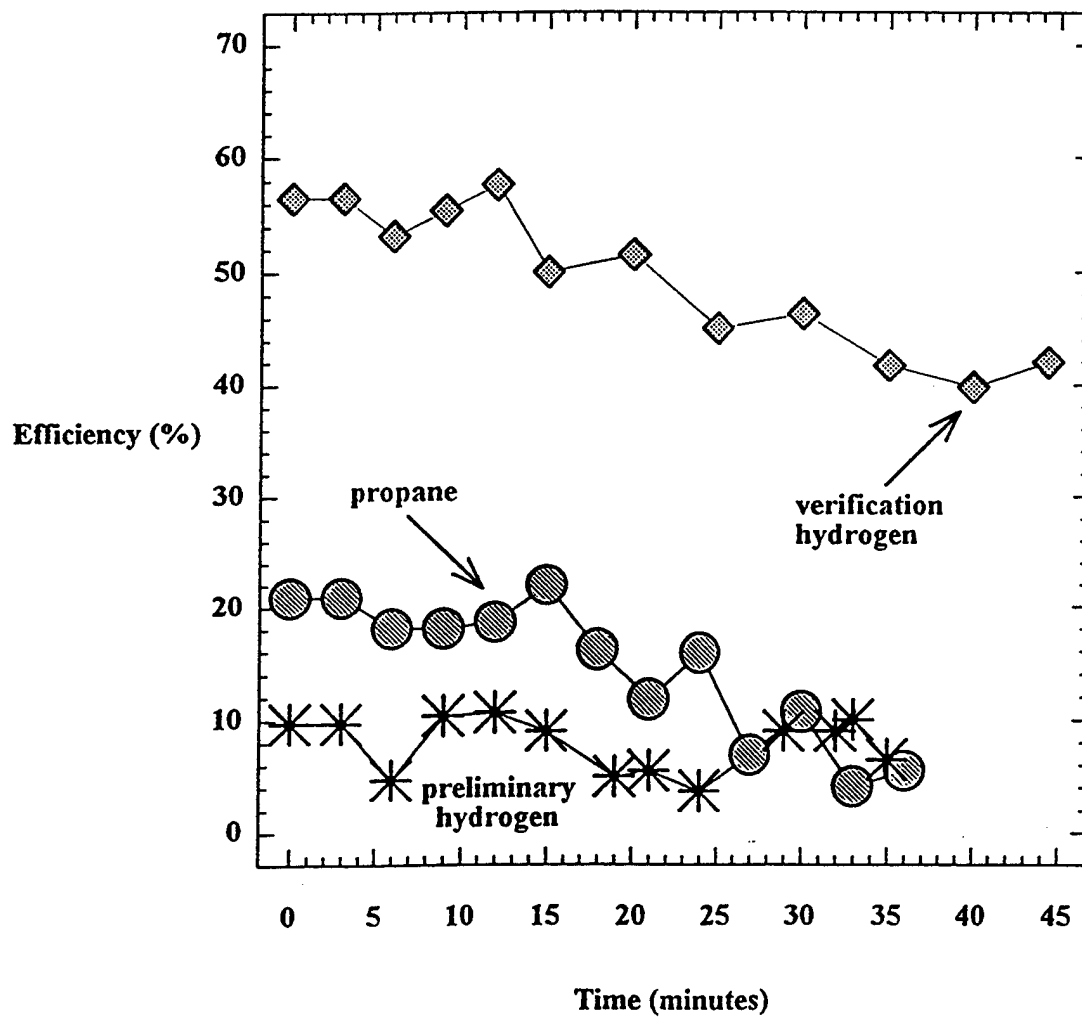


Figure 5. Summary of Efficiencies Measured With M2 Burner: C₃H₈ and H₂

was very disappointing at 7.7% (see Appendix C). The possible sources for the inefficient burns of these experiments was then evaluated, and it was decided to modify the burner design before further experimentation. The four primary issues thought to be responsible for the inefficiencies were (1) the distance between the burner head and kettle bottom, (2) the rate of fuel supply to the burner head, (3) convective heat losses to the ambient, and (4) fuel losses from the air shutter slits. The former two factors have strong relationships to the heat transfer limitations of the burner: the rate of heat supply might be too great for the kettle to absorb, and the flame heat might not be efficiently contacting the kettle thereby diminishing the effective ' ΔT '. These factors would have the net effect of reducing the heat transfer driving force, and increasing the heat losses to ambient within the gap between the kettle and burner head. The last possible source of inefficiencies, the loss of fuel through the air shutter, also directly reduces the amount of usable fuel at the burner head.

1.6.3 Hydrogen Experiments: Table 4 summarizes the subsequent hydrogen-fuel experiments performed after modification of the burner assembly: (1) spacers were added to the mixing section of the burner to elevate the burner head closer to the kettle, (2) an extended hydrogen nozzle was constructed and added to the entrainment section to avoid fuel loss through the air shutter, and (3) the rate of fuel supplied to burner was reduced. The results indicate a marked improvement in burner efficiency from the preliminary experiments, with an average of about 24.4% (3-fold increase). Table 4 shows that the variable with the greatest effect on the efficiency (denoted by '*') was again the shutter opening, which dictates the ratio of hydrogen:air in the burner gas. The other factors, hydrogen flow rate and burner head height, were also notable effects on the performance.

1.6.4 Hydrogen Verification Experiments: The results from the Taguchi experiments were evaluated, and 4 verification experiments were performed. To eliminate the prospect of uncontrolled convective heat losses due to the ambient, the verification experiments were performed in an indoor controlled environment. The experiment in Table 4 which exhibited the highest efficiency of about 36% (experiment #1) was chosen as a basis for the verification runs. The factors which exhibited the greatest effect on the efficiency, flow rate and shutter opening, were then varied in the direction suggested by the Taguchi experiments to further increase the efficiency. Average efficiencies of 44.6, 41.3, 32.9, and 49.0 were measured for these experiments as shown in Appendix C. In addition, efficiencies exceeding 50% were achieved at various points during the experiment, with values fluctuating to 57%.

As suspected, the flow rate of hydrogen has an effect on the efficiency of the burner. When comparing the effect of hydrogen mass flow rate (i.e., rate of energy supply), the higher energy supply rates do not translate to higher efficiencies. This can be seen by comparing experiments 3 and 4 in Table 4 ($0.94 \text{ lb}_m \text{ H}_2/\text{hr}$) and verification experiments 4 and 5 in Appendix C (0.24 and $0.49 \text{ lb}_m \text{ H}_2/\text{hr}$). Figure 6 compares the efficiencies for several mass flow rates. The general trend of Figure 6 is a decrease in efficiency with increasing energy (or mass) flow rate. Note, however, that other factors might also be contributing to the differences displayed, although the experiments did identify the mass

Hydrogen Burner Efficiency With Energy Supply Rate

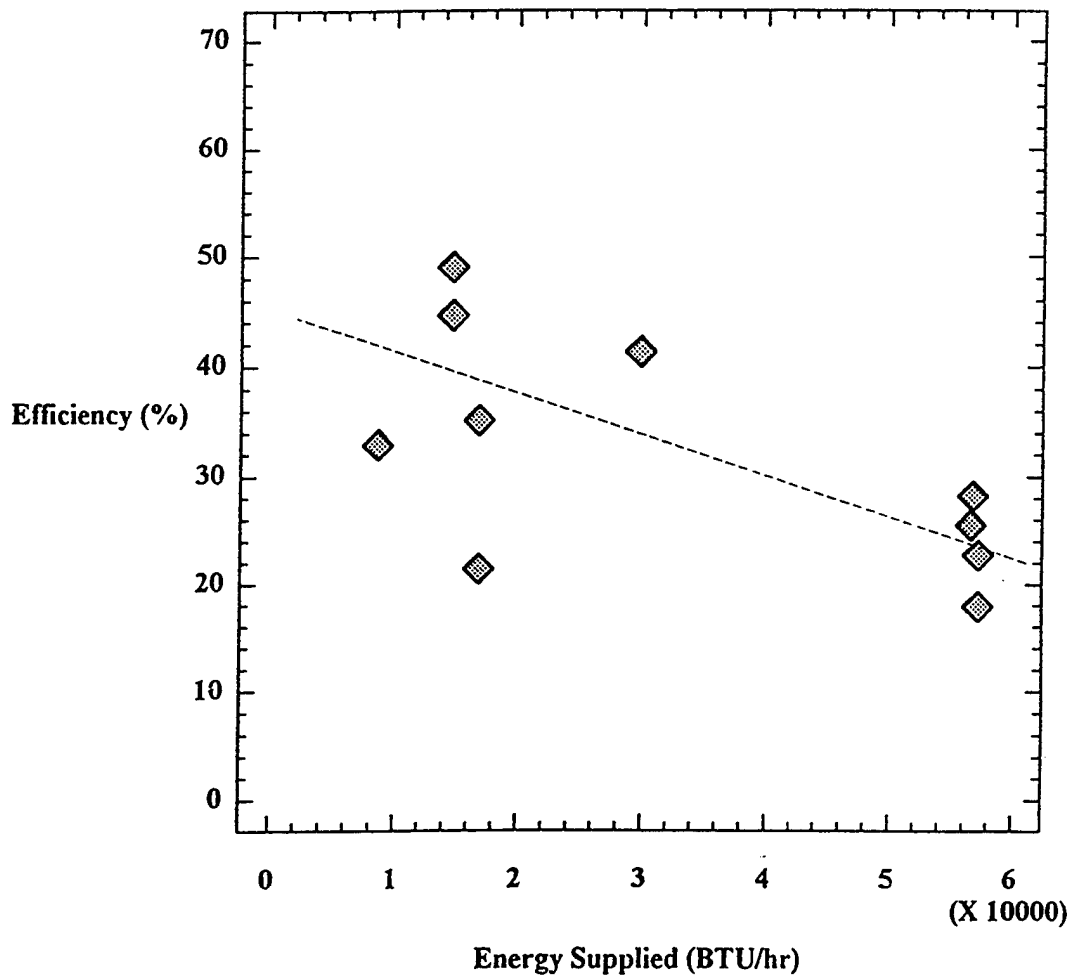


Figure 6. Effect of Energy Supply Rate (Hydrogen Flow Rate) on Burner Efficiency

flow rate as the primary effect. This influence of mass flow rate on efficiency suggests that there is a heat transfer limitation for the burner (i.e., gas-side heat transfer coefficient). Since the Taguchi experiments suggested that a smaller shutter opening produces higher efficiencies, verification experiment #7 was performed with a shutter setting of 'CLOSED', although some air was still being entrained through the air shutter section. Overall, the highest efficiency was measured for hydrogen at 'moderate' flow rates (i.e., not the highest setting) and a higher fuel:air ratio (i.e., less air entrainment) as suggested by the Taguchi experiments.

Since the ambient wind was eliminated for these experiments, it is also suspected that forced convection plays a measurable role in decreasing the efficiency of the burner. This suggests that a redesign of the burner assembly should include appropriate shielding to eliminate forced convection currents into the burner head area. Since the heat transfer coefficient for boiling water is about an order of magnitude larger than those to sub-cooled water, the decrease in efficiency when approaching the boiling point should not be due to the heat transfer limitation on the liquid side of the kettle. The minimization of distance between the burner head and kettle bottom also increased the efficiency of the burner appreciably. This effect is noted in comparing the preliminary hydrogen experiment with an efficiency of 7.7% and a burner head-to-kettle distance of 5", to the verification experiment with an efficiency of 49.0% and a burner head-to-kettle distance of 1". Further modification and refinement of the burner-kettle distance might also increase the efficiency further, since distances shorter than 1" were not tested in this study.

Figure 7 depicts the efficiencies and water temperature for hydrogen verification experiment #7. Note that the efficiency is as high as 57% during the experiment, and the efficiencies seem to drop somewhat as the temperature of the water approaches boiling. This observation could be due to the increasing temperature difference between the hot water/kettle and ambient, thus, an increase in natural convection and radiation heat losses to the environment. This heat loss could be minimized by redesign of the burner assembly with insulation to shield the lower kettle and burner head.

In summary, the efficiency of the burner is greatly influenced by heat transfer limitations. This was demonstrated by the increased efficiency observed when minimizing the distance between the burner head and kettle, for example. An efficiency of hydrogen:air burners in the range 40-50% can be achieved with some modifications to the existing M2 burner, and it is expected that more detailed and rigorous design modifications of the burner could increase this efficiency above 50%. It is believed that such high efficiencies are attainable since radiation heat losses can be as high as 25% [27] and convective heat losses were evident in the experiments as flames were visible outside the cross sectional area of the kettle bottom. It is also suspected that a portion of the increased efficiency is due to the higher fuel:air ratios for hydrogen combustion when compared to propane and gasoline fuel mixtures. As discussed in Progress Report #3 [27], inefficiencies in heat transfer could result from losses due to heat convected away from the heated object by the nitrogen present in air. Consequently, some of the variables which could further increase

Efficiency and Temperature With Time for a Hydrogen-Fueled Burner

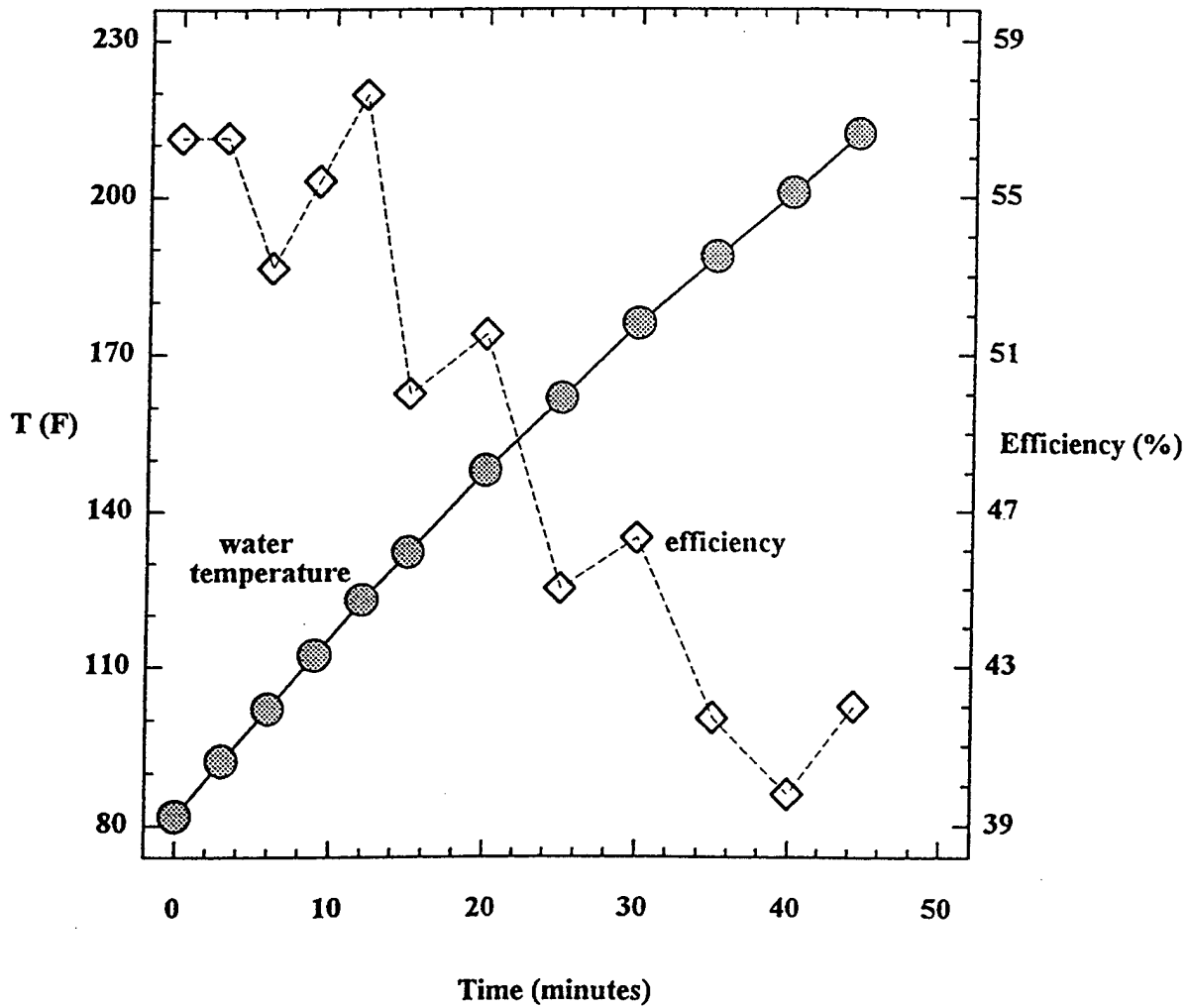


Figure 7. Hydrogen Burner Efficiencies and Water Temperature

the burner efficiency include burner head re-design, baffling to direct the flow (and also increase the heat transfer area), and possibly blackening of the kettle.

1.6.5 Metal-Hydride Burner Experiments: Burner experiments using hydrogen generated from a LaNi_5 hydride bed were performed to evaluate the practicality of using a hydride bed for storage/supply of hydrogen. A summary of several experiments is given in Table 5. Table 5 illustrates that the current hydride bed design is not optimized for use as a hydrogen fuel supply. The expected time for a sustained hydrogen supply to the modified M2 burner did not exceed two minutes when operating at ambient conditions. However, a total burn time of several minutes was achieved. Inadequate heat transfer to the bed during the endothermic desorption reaction is suspected to be the primary resistance to sustained hydrogen desorption. Even when heating the bed to 130°F with heat tape as in experiment #4 with a sustained heat supply of about 400 W (1,366 BTU/hr), the bed cooled considerably (measured at 91°F in the hydrogen overgas, and presumed much cooler within the bed). Since roughly $0.25/\text{lb}_m \text{H}_2/\text{hr}$ was desorbed by the bed during the experiments, and $6,667 \text{ BTU}/\text{lb}_m \text{H}_2$ is required for the endothermic desorption, $0.25 \times 6,667 = 1,667 \text{ BTU/hr}$ is required by the hydride, which is slightly larger than the output of the heat tape. Consequently, the rate of hydrogen desorption was controlled by the rate of heat transfer to the bed which was deficient for a continuous 3 minute burn at 0.25 to $0.5 \text{ lb}_m \text{H}_2/\text{hr}$ (11.2-23.0 liter/min STP). A more efficient heat-transfer bed design would be an integral part of a Phase II effort.

1.6.6 Additional Observations: Some additional observations and side notes regarding the propane and hydrogen-fuel experiments are given below:

- 1.) A water condensate formed on the bottom of the kettle at the beginning of the experiments, but evaporated after the kettle water reached about 120°F . This phenomena is not expected to affect the burner efficiency since an equal and opposite heat was extracted and transferred to the kettle during the water film evaporation and condensation, respectively.
- 2.) Hydrogen and propane flames were visible around the vertical surfaces of the kettle for high flow rates of fuel. This effect is surmised to decrease the overall efficiency of heat transfer to the kettle.
- 3.) No leakage from the press-fit connections of the burner head, spacers, and mixing section were observed. Therefore, fuel losses were assumed to be a negligible contribution to the inefficiencies computed for the burner experiments.
- 4.) The effect of using a 100 mesh screen in the mixing section had little or no effect on the calculated burner efficiencies of hydrogen-fuel. This suggests that the hydrogen:air gases were sufficiently mixed in the mixing and spacer sections.
- 5.) The flame height for the hydrogen burner experiments was approximately 2 inches above the burner head. This height varied with the flow rate of the supplied hydrogen,

TABLE 5 - SUMMARY OF HYDRIDE BURNER EXPERIMENTS

Experiment	delivery pressure, psig	sustained flow rate, l/min stp	sustained flow time (min)	temperature	comments
1	0-10	11.2	2	ambient	temperature dropped to 58F
2	5-10	11.2-23.0	1.5	100F	hot water bath at 100F used: temperature dropped to 67F
3	5-10	11.2	1.5	100F	hot water bath at 100F used: temperature dropped to 70F
4	5-10, started at 110	11.2	2.5	120F	heat tape (400W) used : temperature dropped from 130F to 91F

and was difficult to measure since the hydrogen flame is essentially transparent in the visible light wavelengths.

SECTION 2: SUMMARY OF PHASE I TASKS

The following is a summary of the tasks undertaken in this Phase I effort per the outline established during the kickoff meeting March 18, 1993, and described in Progress Report #1 [34].

Task 1, Literature Review: The literature review surfaced a broad spectrum of materials which might be suitable for hydrogen storage and delivery. Approximately 40 pertinent articles were located and reviewed.

There are several parameters which must be considered in order to select an optimum alloy for specific applications such as food service. For example, safety would be of primary concern both in transportation (low fire hazard in containment vessel ruptures) and while supplying hydrogen (low desorption plateau pressure and therefore the stored gas energy is minimized). In general, it has been stated that hydrogen stored as a metal hydride is safer than gasoline. Reference [35] describes many safety tests performed with LaNi_5 and other metal hydride beds. Their review indicates that metal hydrides were less hazardous in impact tests, and one study concluded that the Index of Explosibility was 0.1 for LaNi_5 (considered a "weak" safety hazard at the time of the study). Although metal hydrides are pyrophoric, the reaction usually occurs at rates dictated by the endothermic desorption kinetics. In addition, exposure to air will generally 'deactivate' the surface where the hydrogen dissociation and re-association occurs during absorption and desorption, respectively. Consequently, the dissociation sites become limited and thus the desorption reaction driving the pyrophoricity is slowed. In contrast, the heating of a gasoline or petro-fuel tank can explode, rather than slow-burn. More specifically, gasoline has an explosion energy 22 times that of hydrogen. Sandrock [32] summarizes safety related properties of hydrogen and gasoline in Table III of his paper.

Cost is another issue when procuring off-the-shelf alloys, but the art of designing inexpensive hydrogen storage materials with specific properties is possible and would also be less expensive in large quantities (e.g., >2500 lb_m).

The cost and safety considerations must also be married with the performance criteria for the hydride (i.e., kinetics and thermodynamics). These issues are thoroughly discussed in Progress Report #3 [27]. In summary, the alloys which seem best suited for use are of the AB_5 variety which include the well-documented LaNi_5 material, and numerous other "mischmetal" derivatives. The LaNi_5 alloy was subsequently chosen and 2 kg was purchased from Ergenics, Inc., for burner studies.

Task 2, Establish System Requirements: As stated in the Bi-monthly Report #1 [34], the heating load will be the primary design parameter. Currently, the M2 gasoline-burner operates at 60,000 BTU/hr with an efficiency of 25%. Tables 1 and 2 summarize a system

based on the 50% efficiency measured in this effort. Sections 1.2 and 1.3 also elaborate on the system requirements and design of the experimental burner used for the efficiency studies.

Task 3, Design of a Hydrogen Fueled Kitchen: The design parameters established for a hydrogen fueled kitchen are summarized in Table 1. The total weight of the hydrogen burner systems are estimated to be about 1,500 lb_m in addition to the kitchen frame support hardware. After initial materials costs, the fuel costs will be for H₂ gas alone (\$25/lb_m): 15 lb_m for 6 burners operating for 5 hours at 50% efficiency will cost \$375.

Task 4, Proof-of-Concept Experiments: Efficiency studies were performed with propane and hydrogen as described in sections 1.5 and 1.6. In addition to these studies a 3 minute burn of hydrogen evolved from a metal hydride was investigated. Approximately 1.5 kg of LaNi₅ was loaded into a 1 liter cylinder and activated by heating and pulling a vacuum on the system. Then the material was loaded with hydrogen by charging in about ten (10) 500 psia increments. The total quantity of hydrogen absorbed by the bed was 21 g, or the equivalent of 235 liters (STP). To use this hydrogen for burner fuel, heating tape was wrapped around the cylinder, or the cylinder was immersed in hot water, and hydrogen was allowed to flow out of the cylinder and ignited at the burner head. The flow rate of the gas desorbing from the hydride bed was adjusted between flow rates of 0.1 and 0.5 lb_m H₂/hr, which was dependent upon the rate of heat supply to the bed. The desorption reaction is highly endothermic, and the desorption kinetics and subsequent hydrogen supply slowed considerably as the bed cooled. The temperature of hydrogen gas in equilibrium with the hydride approached 50°F after a short period of time (1-2 minutes), so the temperature of the hydride bed itself was believed to be somewhat lower. A summary of these experiments is given in Table 5.

Since the endothermic reaction of hydrogen desorption cools the hydride bed, thus slowing the kinetics of the delivery, future designs will require heat transfer optimization to enhance the heat exchange of the desorbing bed with ambient. The one liter cylinder is not an optimum configuration for holding the hydride powder since the depth of the bed is approximately 1 inch at center (when the cylinder is positioned horizontally) and thermal conductivity within the bed and cylinder-air heat transfer limitations become appreciable. An optimum design would require extended heat transfer area, the use of waste heat from the burner or extraction of heat for use in refrigeration processes, and reduced-depth hydride beds.

Task 5, System Drawings and Reports: Bi-monthly reports were distributed for the effort and drawings illustrating the benchtop prototype burner are included in this report (see Figures 1 and 2).

SECTION 3: DISCUSSION OF RESULTS

This Phase I effort has established the feasibility of a hydrogen fueled kitchen for the Army. Energy efficiencies with hydrogen were produced in the range 40-50%, and in a Phase II effort additional increases in the efficiency are expected. The prototype burner developed is of a relatively simple light-weight design, operating with compressed hydrogen gas or gas stored on a metal hydride bed. The results of experiments with hydrogen and propane indicate that heat transfer factors and burner head design could play a very important role in improved burner designs. It was also concluded that a more rigorous hydride bed design is necessary to overcome heat transfer limitations and supply hydrogen at sustained flow rates as discussed in sections 1.6 and 1.7.

For example, consider a hydride bed providing 0.5 lb_m H₂/hr (1.9 g-mole H₂/min), or 30,500 BTU/hr of energy, for a burner operating at 50% efficiency (15,000 BTU/hr usable heat). The endothermic reaction of hydrogen desorption requires about 6,600 BTU/lb_m H₂, or at 0.5 lb_m H₂/hr this equates to 3,300 BTU/hr. Thus, (3,300/30,500) x 100% = 11% of the available energy of the hydrogen combustion reaction could be used to heat the hydride bed, leaving 89% for usable heat in the kitchen operation. Figure 8 summarizes the advanced concept for the utilization of waste heat from the burner to assist in the desorption of hydrogen from a metal-hydride bed.

Another advanced concept could utilize the heat extracted from the environment during the desorption of hydrogen for refrigeration. For example, since the desorption reaction requires about 6,600 BTU/lb_m H₂, a total cooling energy of 6,600 BTU/lb_m H₂ x 0.5 lb_m H₂/hr x 5 hour operation/burner x 6 burners = 99,000 BTU is extracted from the environment. For example, if the refrigeration process operates at 75% efficiency, a total of 99,000 BTU x 75% = 74,250 BTU is available which could be used to cool water from 120°F to 70°F. Thus, 74,250 BTU / (1 BTU/lb_m°F)(120°F-70°F) = 1,485 lb_m water, or 178 gallons, could be cooled during the 5 hour kitchen operation.

The size and weight of an efficient hydride bed can be estimated by accounting for the thermal conductivity and convective heat transfer effects. For LaNi₅, the thermal conductivity is 3.15x10⁻⁴ kcal/m-s-K, and a typical free-convection heat transfer coefficient for air is 2.8x10⁻³ kcal/m²-s-K. Assuming a hydride bed depth of 0.25" (0.00635 m), and a temperature difference of 50°C between the surroundings and the bed, the overall heat transfer coefficient can be estimated by:

$$U = \frac{1}{\frac{1}{h} + \frac{\Delta x}{k}} = \frac{1}{\frac{1}{2.8 \times 10^{-3}} + \frac{0.00635}{3.15 \times 10^{-4}}} = 2.65 \times 10^{-3} \frac{\text{kcal}}{\text{m}^2 \text{s}^\circ \text{K}} \quad [\text{Eq. 8}]$$

and the limiting rate of heat absorption by the hydride bed is then

$$Q_{bed} = AU\Delta T = A \cdot (2.65 \times 10^{-3}) \cdot (50) = 0.133 \cdot A \frac{\text{kcal}}{\text{m}^2 \text{s}} \quad [\text{Eq. 9}]$$

Since 3,300 BTU/hr (0.233 kcal/s) of heat is required (Q_{req}) by the hydride for the desorption reaction, the cross sectional area of the bed can be estimated as $A=Q_{req}/Q_{bed}=0.233/0.133=1.75 \text{ m}^2$ (2713 in²). Consequently, a bed having the dimensions of about 4.5 feet x 4.5 feet containing a 1/4" deep bed of hydride would be required. The resulting volume of the bed is $17,500 \text{ cm}^2 \times (0.25") \times (2.54 \text{ cm/in}) = 11,100 \text{ cm}^3$ (0.4 ft³), or $(11,100 \text{ cm}^3) \times (4.5\text{g/cm}^3)=50 \text{ kg LaNi}_5$. This quantity of LaNi_5 will absorb about 700 g H_2 (1.5 lb_m), and supply a burner at 0.5 lb_m/hr for 3 hours. In order to facilitate a simple activation processes, the hydride bed, or 'tray', could be comprised of several modules containing lesser amounts of hydride (as illustrated in Figure 8). In order to provide a conductive heat transfer path through the hydride bed, conductive dilution materials such as aluminum might also be mixed with the metal hydride powder. Research has been performed to confirm the increased desorption kinetics of such techniques [36,37].

A Phase II effort would focus on increasing the burner efficiencies from this Phase I effort, and in addition, develop field-usable prototypes. Some specific areas of Phase II development include: (1) redesign of burner head to eliminate flame extension around the kettle and heat convective losses around the burner head, (2) redesign of the burner head to direct a flame with high velocity across the bottom of kettle, possibly utilizing baffles which would also increase the heat transfer area, (3) blacken surfaces where possible to reduce radiation heat transfer losses, (4) insulate or shelter the flame and burner head from ambient to decrease convective heat losses, (5) determine optimum energy supply rates for the hydrogen fuel, and (6) develop efficient hydride storage beds to increase heat transfer between hydride and ambient during desorption and reloading. Mainstream has expertise and proven successes in heat transfer designs, fluid flow, hardware design, metal hydrides, and hydrogen handling, and would extend the technological boundaries of commercial and military hydrogen-fuel applications through a Phase II effort.

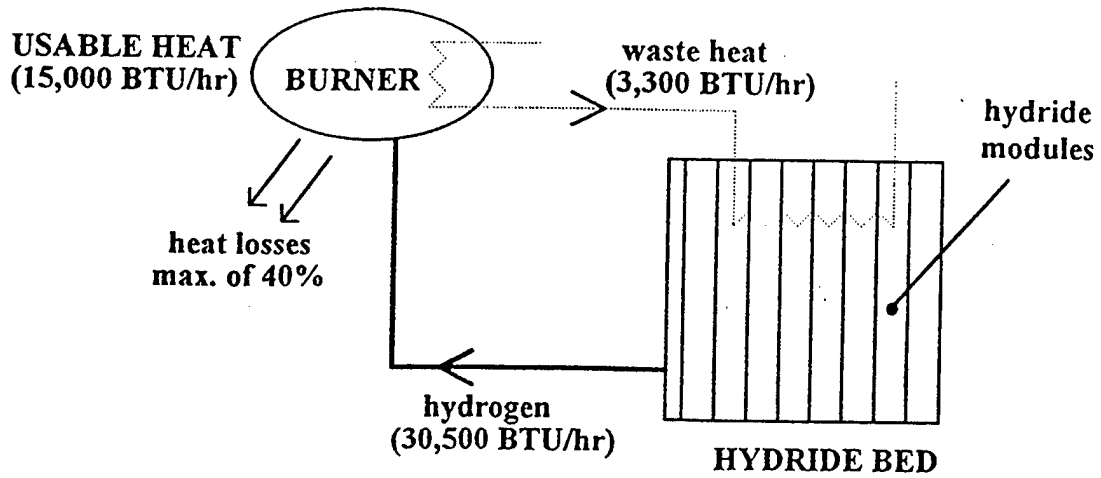


Figure 8a. The Use of Waste Burner Heat for Hydride Desorption

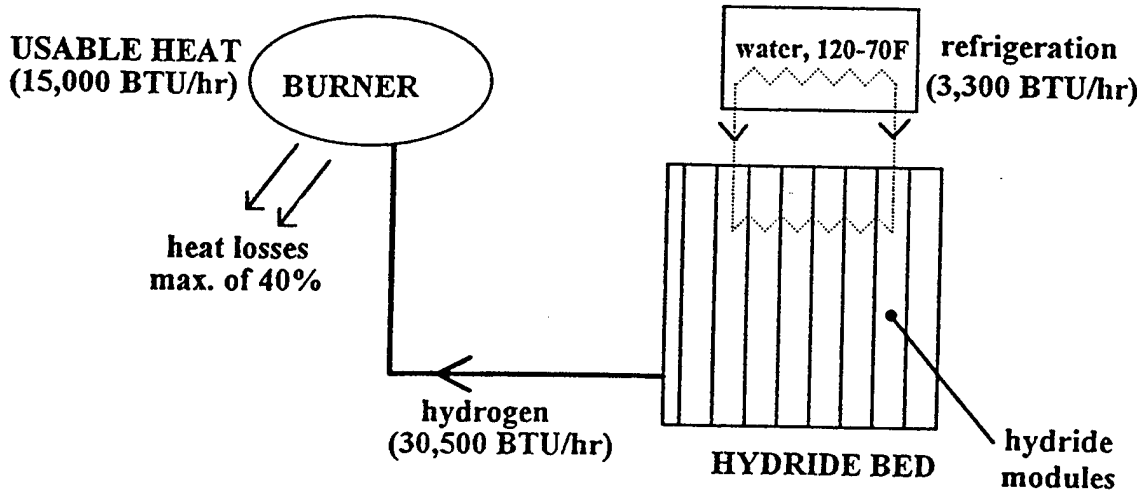


Figure 8b. The Use of Hydride Heat-of-Desorption for Refrigeration

This document reports research undertaken at the U.S. Army Soldier and Biological Chemical Command, Soldier Systems Center, and has been assigned No. NATICK/TR-99/020 in a series of reports approved for publication.

SECTION 4: REFERENCES

1. Barile, R.G., Littlefield, M.D., Parrish, C., Linsley, J.N., and Bowman, T.E. "Thermal Storage Devices for Load Leveling of a Two-Phase Thermal Transport System," NASA Contract No. NASA-10-10980, Kennedy Space Center, FL, September, 1985.
2. Scaringe, R. P., "Development of a Prototype Rotary-Vane Compressor for Microclimate Cooling Applications, "Army Natick RD&E Center Final Report, December 1991.
3. Gui, F., Scaringe, R. P., "Design and Fabrication of a Man-Portable Liquid Cooling Backpack," Army Natick RD&E Center Phase IIB Final Report, May 1992.
4. Scaringe, R. P., Cadenhead, J., "Design and Fabrication of a Man-Portable Liquid Cooling Backpack," Army Natick RD&E Center Phase I Final Report, 1991.
5. Scaringe, R. P., Silvestri, J. J., "Design and Fabrication of a Man-Portable Air Cooling Backpack," Army Natick RD&E Center Phase I Final Report, 1991.
6. Rahman, M. M., Scaringe, R. P., Cadenhead, J., "Design and of a Brayton Cycle Backpack Cooling System," Army Natick RD&E Center Final Report, 1992.
7. Silvestri, J.J., Scaringe, R.P., Grzyll, L.R. and Swanson, T., "Performance of a Hybrid Chemical-Mechanical Heat Pump," Presented at the 1990 Intersociety Energy Conversion Engineering Conference, August 12-17, 1990, Reno, NV.
8. Silvestri, J.J., and Buckman, J.A., "Advanced Heat Pump Modeling", Presented at the 1990 Intersociety Energy Conversion Engineering Conference, August 12-17, 1990, Reno, NV.
9. Silvestri, J.J., Grzyll, L. R., and Schantz, I., "Thermal Response of TXV-Controlled Heat Pump Systems Operating with Refrigerant Mixtures," Submitted for Presentation at the 1990 IECEC in Reno, Nevada.
10. Silvestri, J.J., Scaringe, R.P., Buckman, J.A., Mahefkey, E.T. and Leland, J., "Thermal Response of Heat Pump Augmented Spacecraft Heat Rejection Systems," ASME Winter Annual Meeting, San Francisco, CA, December 1989.
11. Scaringe, R.P., Buckman, J.A., Grzyll, L.R., Mahefkey, E.T. and Leland, J., "Heat Pump Augmented Spacecraft Heat Rejection Systems," Journal of Spacecraft and Rockets, AIAA, December 1989.
12. Scaringe, R.P., Grzyll, J.A., and Silvestri, J.J., "Modular Chemical/Mechanical Heat Pump for Spacecraft Thermal Bus Applications Final Report," MEC Report # 33589011, August, 1989.
13. Scaringe, R.P., Buckman, J.A., Grzyll, L.R., Mahefkey, E.T. and Leland, J., "Investigation of Advanced Heat Pump Augmented Spacecraft Heat Rejection Systems," AIAA Paper 89-0072, 27th Aerospace Sciences Meeting, AIAA, January 9-12, 1989, Reno, Nevada
14. Scaringe, R.P., and Mahefkey, E.T., "Preliminary Investigation of an Integrated Heat Pump Spacecraft Thermal Management Systems," ASME Winter Annual Meeting, Chicago, IL, December 1988.
15. Scaringe, R.P., Buckman, J.J. and Grzyll, J.A., " Heat Pump Thermal Transport Loop for Spacecraft Applications Final Report," MEC Report # 33588004, December, 1988.

16. Scaringe, R.P., Buckman, J.J. and, Grzyll, L.R., "Development of A General Simulation Program for Spacecraft Applications Final Report, "Department of the Air Force, Aeronautical Systems Division, Wright-Patterson AFB, Contract F33615-87-C-2841, MEC Report # 33588003, July 1988.
17. Scaringe, R.P., "Preliminary Investigation of Advanced Heat Pump Augmented Spacecraft Heat Rejection Systems, "International Symposium on Thermal Problems in Space-Based Systems," HTD-VOL 83, ASME Winter Annual Meeting, December 1987.
18. Scaringe, R.P., "Factors Affecting Stirling Cycle Heat Pump Design," Florida Academy of Science, April 1983, Melbourne, Florida.
19. Silvestri, J.J., and Scaringe, R. P., "Advanced Heat Pump Augmented Spacecraft Heat Rejection System," Monthly Status Report # 18, AFWAL/POOS-3, Dayton, OH, May 1990.
20. Grzyll, L.R., Scaringe, R.P., and Silvestri, J.J., "Advanced Heat Pump Augmented Spacecraft Heat Rejection System Final Report," AFWAL/POOS-3, Dayton, OH, 1991.
21. Scaringe, R.P., Grzyll, J.A., Buckman, J.A., Silvestri, J.J., and Barthel-Rosa, L., "Improved System for Scape Suit Heating Contract Final Report," MEC Report # 33589007, August, 1989.
22. Back, D.D., The Kinetics of Hydrogen Sorption by Palladium and Palladium Alloys, Internal Technical Report, EG&G Mound Applied Technologies, 1989.
23. Back, D.D., Schleitweiler, P., Walburg, T.F., Werkmeister, D.W., Stresses Induced by the Hydriding of Metal Compacts, Storage Science Meeting, Westinghouse Savannah River Company, Savannah River, SC, May, 1993.
24. Back, D.D., Werkmeister, D.W., Ultrasonic Measurements on Pd Compacts (Green and Hydrided), Storage Science Meeting, Westinghouse Savannah River Company, Savannah River, SC, May, 1991.
25. Back, D.D., Tritium Capture Without Conversion to Water, DoE TTP DAO314-06 Progress Reports, 1990-1993.
26. Back, D.D., Palladium and Palladium Alloy Hydrides for Use in Chemical Pumps, Final Project Report for Los Alamos National Laboratory, 1990.
27. Back, D.D., Demonstration of the Use of Hydrogen Fuel for Food Service (Progress Report #3), SBIR Phase I Contract DAAK60-93-C-0017, Mainstream Engineering Corporation, Rockledge, FL, 1993.
28. McCabe, W.K., and J.C. Smith, Unit Operations of Chemical Engineering, 3rd ed., McGraw-Hill Book Company, 1976.
29. Perry, R.H., and C.H. Chilton, Chemical Engineers' Handbook (5th ed.), McGraw-Hill, 1973.
30. Lange, N.A., Handbook of Chemistry, 10th ed., McGraw-Hill Book Company, 1961.
31. Bird, R.B., W.E. Stewart, and E.N Lightfoot, Transport Phenomena, John Wiley and Sons, 1961.
32. Sandrock, G. D., Hydrogen Storage, presented at the Hydrogen Energy Symposium, Stockholm, Sweden, 1981.
33. ReVelle, J.B., The New Quality Technology: An Introduction to Quality Function Deployment (QFD) and the Taguchi Methods, Hughes Aircraft Company, 1990.

34. Back, D.D., Demonstration of the Use of Hydrogen Fuel for Food Service (Progress Report #1), SBIR Phase I Contract DAAK60-93-C-0017, Mainstream Engineering Corporation, Rockledge, FL, 1993.
35. Donnelly, J.J., W.C. Greayer, R.J. Nichols, and W.J.D. Escher, Study of Hydrogen-Powered Versus Battery-Powered Automobiles, Department of Energy Report ATR-79(7759)-1(Vol.2), Contract # EM-78-C-03-2184, 1979.
36. Goudy, A.J., D.G. Stokes, and J.A. Gazzillo, The Effect of Heat Transfer on the Desorption Kinetics of LaNi_5H_6 , *J. Less-Common Met.*, 91, p 149, 1983.
37. Goudy, A.J., and R.A. Wallingford, Desorption Kinetics of LaNi_5 , $\text{LaNi}_{4.7}\text{Al}_{0.3}$, $(\text{CFM})\text{Ni}_5$, and $\text{MNi}_{4.5}\text{Al}_{0.5}$ Hydrides, *J. Less-Common Met.*, 99, p 249, 1984.

Appendix

Raw Data For Propane And Hydrogen Efficiency Studies

Propane Experiments (1 of 4)

BURNER DATA: PROPANE EXPERIMENTS

RUN: experiment#1: factor levels 1-1-1: 7/28/93

Pressure	20.7	SG	1.5311	
Flow (scfh)	5.0	amb. T	100.0	F
mass	40.0	Q Value	19929	BTU/lb
Flow V =	0.00129579 cu.ft./s	AVG. EFF.	12.1	
Flow m =	0.70869577 lb/hr	STD.DEV.	3.7	
Q supplied =	14,124 BTU/hr	LUMP EFF.	12.1	

Time (min)	Temp (F)	Q(t)	Q(t)/t	Q(t)-Th.	Effic.(%)
0	95	0.0	0.0	0.0	0.0
6	101.2	248.0	2480.0	1412.4	17.6
12	105.2	160.0	1600.0	1412.4	11.3
18	111.8	264.0	2640.0	1412.4	18.7
24	117.2	216.0	2160.0	1412.4	15.3
30	122.6	216.0	2160.0	1412.4	15.3
36	126.8	168.0	1680.0	1412.4	11.9
42	131.6	192.0	1920.0	1412.4	13.6
48	135.4	152.0	1520.0	1412.4	10.8
54	139.2	152.0	1520.0	1412.4	10.8
60	142	112.0	1120.0	1412.4	7.9
66	145.6	144.0	1440.0	1412.4	10.2
72	149	136.0	1360.0	1412.4	9.6
78	150.6	64.0	640.0	1412.4	4.5

Q(t) is the heat utilized by the 40 pounds of water since the previous measurement (BTU)

Q(t)/t is the rate of heat supplied to the water since the last measurement (BTU/hr)

Q(t)-Th. is the theoretical rate of heat supplied by the fuel:air mixture for the same time period (BTU/hr)

Effic.(%) is the efficiency of the burner for each time interval

BURNER DATA: PROPANE EXPERIMENTS

RUN: experiment#2: factor levels 1-2-2: 7/28/93

Pressure	20.7	SG	1.5311	
Flow (scfh)	20.0	amb. T	88.4	F
mass	40.0	Q Value	19929	BTU/lb
Flow V =	0.00523771	cu.ft./s	AVG. EFF.	14.1
Flow m =	2.92520092	lb/hr	STD.DEV.	6.0
Q supplied =	58,296	BTU/hr	LUMP EFF.	14.1

Time (min)	Temp (F)	Q(t)	Q(t)/t	Q(t)-Th.	Effic.(%)
0	89	0.0	0.0	0.0	0.0
3	104.2	608.0	12160.0	2914.8	20.9
6	117.4	528.0	10560.0	2914.8	18.1
9	130.6	528.0	10560.0	2914.8	18.1
12	144.2	544.0	10880.0	2914.8	18.7
15	160.2	640.0	12800.0	2914.8	22.0
18	172	472.0	9440.0	2914.8	16.2
21	180.6	344.0	6880.0	2914.8	11.8
24	192.2	464.0	9280.0	2914.8	15.9
27	197.2	200.0	4000.0	2914.8	6.9
30	205	312.0	6240.0	2914.8	10.7
33	208	120.0	2400.0	2914.8	4.1
36	212	160.0	3200.0	2914.8	5.5

BURNER DATA: PROPANE EXPERIMENTS

RUN: experiment#3: factor levels 2-1-2: 7/29/93

Pressure	20.7	SG	1.5311	
Flow (scfh)	20.0	amb. T	83.6	F
mass	40.0	Q Value	19929	BTU/lb
Flow V =	0.00526078	cu.ft./s	AVG. EFF.	8.6
Flow m =	2.96403071	lb/hr	STD.DEV.	3.9
Q supplied =	59,070	BTU/hr	LUMP EFF.	8.6

Time (min)	Temp (F)	Q(t)	Q(t)/t	Q(t)-Th.	Effic.(%)
0	84.4	0.0	0.0	0.0	0.0
3	93	344.0	6880.0	2953.5	11.6
6	102	360.0	7200.0	2953.5	12.2
9	109.8	312.0	6240.0	2953.5	10.6
12	120.2	416.0	8320.0	2953.5	14.1
15	129.6	376.0	7520.0	2953.5	12.7
18	139	376.0	7520.0	2953.5	12.7
21	149.4	416.0	8320.0	2953.5	14.1
24	158	344.0	6880.0	2953.5	11.6
27	164	240.0	4800.0	2953.5	8.1
30	169.8	232.0	4640.0	2953.5	7.9
33	177.4	304.0	6080.0	2953.5	10.3
36	181.2	152.0	3040.0	2953.5	5.1
39	187.2	240.0	4800.0	2953.5	8.1
42	190.4	128.0	2560.0	2953.5	4.3
45	192	64.0	1280.0	2953.5	2.2
48	196	160.0	3200.0	2953.5	5.4
51	203	280.0	5600.0	2953.5	9.5
54	207	160.0	3200.0	2953.5	5.4
57	210.4	136.0	2720.0	2953.5	4.6
60	211.8	56.0	1120.0	2953.5	1.9

BURNER DATA: PROPANE EXPERIMENTS

RUN: experiment#4: factor levels 2-2-1: 7/28/93

Pressure	20.7	SG	1.5311	
Flow (scfh)	5.0	amb. T	100.0	F
mass	40.0	Q Value	19929	BTU/lb
Flow V =	0.00129579	cu.ft./s		
Flow m =	0.70869577	lb/hr		
Q supplied =	14,124	BTU/hr		
		AVG. EFF.		11.0
		STD.DEV.		3.9
		LUMP EFF.		10.6

Time (min)	Temp (F)	Q(t)	Q(t)/t	Q(t)-Th.	Effic.(%)
0	86.6	0.0	0.0	0.0	0.0
3	88.6	80.0	1600.0	706.2	11.3
6	89.8	48.0	960.0	706.2	6.8
9	91.8	80.0	1600.0	706.2	11.3
12	93	48.0	960.0	706.2	6.8
15	95.2	88.0	1760.0	706.2	12.5
18	96.8	64.0	1280.0	706.2	9.1
21	99	88.0	1760.0	706.2	12.5
31	105.4	256.0	1536.0	2353.9	10.9
41	111.5	244.0	1464.0	2353.9	10.4
51	117.2	228.0	1368.0	2353.9	9.7
61	123	232.0	1392.0	2353.9	9.9
67	128.2	208.0	2080.0	1412.4	14.7
71	133.2	200.0	3000.0	941.6	21.2
81	137.2	160.0	960.0	2353.9	6.8

PRELIMINARY HYDROGEN EXPERIMENTS

RUN: experiment#1: factor levels 2-1-2 (see propane exp'ts): 7/27/93

Pressure	20.7	SG	0.06944444
Flow (scfh)	25.0	amb. T	95.0 F
mass	39.0	Q Value	60958.0 BTU/lb
Flow V =	0.03055883 cu.ft./s	AVG. EFF.	7.8
Flow m =	0.76479817 lb/hr	STD.DEV.	2.6
Q supplied =	46,621 BTU/hr	LUMP EFF.	7.7

Time (min)	Temp (F)	Q(t)	Q(t)/t	Q(t)-Th.	Effic.(%)
0	99.2	0.0	0.0	0.0	0.0
3	105	226.2	4524.0	2331.0	9.7
6	107.8	109.2	2184.0	2331.0	4.7
9	114	241.8	4836.0	2331.0	10.4
12	120.4	249.6	4992.0	2331.0	10.7
15	125.8	210.6	4212.0	2331.0	9.0
19	129.8	156.0	2340.0	3108.0	5.0
21	132	85.8	2574.0	1554.0	5.5
24	134.2	85.8	1716.0	2331.0	3.7
29	143.2	351.0	4212.0	3885.0	9.0
32	148.6	210.6	4212.0	2331.0	9.0
33	150.6	78.0	4680.0	777.0	10.0
35	153.2	101.4	3042.0	1554.0	6.5

(modified) BURNER DATA: HYDROGEN

RUN: experiment#1: factor levels 1-1-1: 8/16/93

Rotameter	10.0				
Pressure	16.2	psia			
Flow (scfh)	48.7	H2	SG	0.06944444	
mass	40.0		amb. T	87.0	F
			Q Value	60958.0	BTU/lb
Flow V =	0.0139687	cu.ft./s			
Flow m =	0.2775981	lb/hr		AVG. EFF.	35.1
Q supplied =	16,922	BTU/hr		STD.DEV.	9.6
				LUMP EFF.	35.5

Time (min)	Temp (F)	Q(t)	Q(t)/t	Q(t)-Th.	Effic.(%)
0	87	0.0	0.0	0.0	0.0
3	98.8	472.0	9440.0	846.1	55.8
6	105.8	280.0	5600.0	846.1	33.1
9	117	448.0	8960.0	846.1	52.9
12	127.2	408.0	8160.0	846.1	48.2
15	131.8	184.0	3680.0	846.1	21.7
18	141.4	384.0	7680.0	846.1	45.4
21	145.8	176.0	3520.0	846.1	20.8
24	152.4	264.0	5280.0	846.1	31.2
27	160.4	320.0	6400.0	846.1	37.8
30	167.8	296.0	5920.0	846.1	35.0
33	174.8	280.0	5600.0	846.1	33.1
36	180.6	232.0	4640.0	846.1	27.4
39	188.4	312.0	6240.0	846.1	36.9
42	195.8	296.0	5920.0	846.1	35.0
45	202.4	264.0	5280.0	846.1	31.2
48	209.6	288.0	5760.0	846.1	34.0
50	212	96.0	2880.0	564.1	17.0

Hydrogen Experiments (2 of 4)

(modified) BURNER DATA: HYDROGEN

RUN: experiment#2: factor levels 1-2-2: 8/16/93

Rotameter	20.0	(N064-63ST)			
Pressure	22.7	psia	SG	0.06944444	
Flow (scfh)	98.7	H2	amb. T	85.0	F
mass	40.0		Q Value	60958.0	BTU/lb
Flow V =	0.03360247	cu.ft./s	AVG. EFF.		22.7
Flow m =	0.9391464	lb/hr	STD.DEV.		8.0
Q supplied =	57,248	BTU/hr	LUMP EFF.		23.0

Time (t)	Temp (F)	Q(t)	Q(t)/t	Q(t)-Th.	Effic.(%)
0	85.6	0.0	0.0	0.0	0.0
3	105.6	800.0	16000.0	2862.4	27.9
6	121	616.0	12320.0	2862.4	21.5
9	144	920.0	18400.0	2862.4	32.1
12	168	960.0	19200.0	2862.4	33.5
15	180	480.0	9600.0	2862.4	16.8
18	190	400.0	8000.0	2862.4	14.0
21	205	600.0	12000.0	2862.4	21.0
23	212	280.0	8400.0	1908.3	14.7

Hydrogen Experiments (3 of 4)

(modified) BURNER DATA: HYDROGEN

RUN: experiment#3: factor levels 2-1-2: 8/16/93

Rotameter	20.0				
Pressure	22.7	psia		SG	0.06944444
Flow (scfh)	98.7	H2		amb. T	85.0 F
mass	40.0			Q Value	60958.0 BTU/lb
Flow V =	0.03360247	cu.ft./s		AVG. EFF.	17.9
Flow m =	0.9391464	lb/hr		STD.DEV.	4.3
Q supplied =	57,248	BTU/hr		LUMP EFF.	18.0

Time (min)	Temp (F)	Q(t)	Q(t)/t	Q(t)-Th.	Effic.(%)
0	87.6	0.0	0.0	0.0	0.0
3	103.8	648.0	12960.0	2862.4	22.6
6	116.4	504.0	10080.0	2862.4	17.6
9	131	584.0	11680.0	2862.4	20.4
12	145	560.0	11200.0	2862.4	19.6
15	158.6	544.0	10880.0	2862.4	19.0
18	176.2	704.0	14080.0	2862.4	24.6
21	183.8	304.0	6080.0	2862.4	10.6
24	196	488.0	9760.0	2862.4	17.0
27	205	360.0	7200.0	2862.4	12.6
29	212	280.0	8400.0	1908.3	14.7

VERIFICATION HYDROGEN EXPERIMENTS

RUN: verification 4: factor levels 1-1-1: 9/27/93

Rotameter	10.0				
Pressure	14.7	psia	SG	0.06944444	
Flow (scfh)	48.7	H2	amb. T	84.5	F
mass	40.0		Q Value	60958.0	BTU/lb
Flow V =	0.01333681	cu.ft./s	AVG. EFF.		44.6
Flow m =	0.241604	lb/hr	STD.DEV.		9.2
Q supplied =	14,728	BTU/hr	LUMP EFF.		45.5

Time (min)	Temp (F)	Q(t)	Q(t)/t	Q(t)-Th.	Effic.(%)
0	85	0.0	0.0	0.0	0.0
3	94.2	368.0	7360.0	736.4	50.0
6	103.8	384.0	7680.0	736.4	52.1
9	114	408.0	8160.0	736.4	55.4
12	123	360.0	7200.0	736.4	48.9
15	131.6	344.0	6880.0	736.4	46.7
20	145.4	552.0	6624.0	1227.3	45.0
25	158.8	536.0	6432.0	1227.3	43.7
30	171.8	520.0	6240.0	1227.3	42.4
35	185.8	560.0	6720.0	1227.3	45.6
40	196.8	440.0	5280.0	1227.3	35.9
45	204.6	312.0	3744.0	1227.3	25.4
49.1	212	296.0	4331.7	1006.4	29.4

VERIFICATION HYDROGEN EXPERIMENTS

RUN: verification 5: factor levels 1-1-2: 9/27/93

Rotameter	20.0				
Pressure	14.7	psia		SG	0.06944444
Flow (scfh)	98.7	H2		amb. T	84.5 F
mass	40.0			Q Value	60958.0 BTU/lb
Flow V =	0.02705305	cu.ft./s		AVG. EFF.	41.3
Flow m =	0.49008165	lb/hr		STD.DEV.	8.4
Q supplied =	29,874	BTU/hr		LUMP EFF.	41.3

Time (min)	Temp (F)	Q(t)	Q(t)/t	Q(t)-Th.	Effic.(%)
0	87	0.0	0.0	0.0	0.0
3	105.2	728.0	14560.0	1493.7	48.7
6	125.4	808.0	16160.0	1493.7	54.1
9	139	544.0	10880.0	1493.7	36.4
12	153	560.0	11200.0	1493.7	37.5
15	168	600.0	12000.0	1493.7	40.2
18	185	680.0	13600.0	1493.7	45.5
21	198	520.0	10400.0	1493.7	34.8
24	210.4	496.0	9920.0	1493.7	33.2
24.49	212	64.0	7836.7	244.0	26.2

VERIFICATION HYDROGEN EXPERIMENTS

RUN: verification 6: factor levels 1-1-3: 9/27/93

Rotameter	6.0				
Pressure	14.7	psia	SG	0.06944444	
Flow (scfh)	28.6	H2	amb. T	84.5	F
mass	40.0		Q Value	60958.0	BTU/lb
Flow V =	0.00785031	cu.ft./s	AVG. EFF.		32.9
Flow m =	0.14221294	lb/hr	STD.DEV.		7.0
Q supplied =	8,669	BTU/hr	LUMP EFF.		31.9

Time (min)	Temp (F)	Q(t)	Q(t)/t	Q(t)-Th.	Effic.(%)
0	86.4	0.0	0.0	0.0	0.0
10	103	664.0	3984.0	1444.8	46.0
20	116	520.0	3120.0	1444.8	36.0
30	130	560.0	3360.0	1444.8	38.8
40	141.2	448.0	2688.0	1444.8	31.0
50	152.2	440.0	2640.0	1444.8	30.5
60	161.8	384.0	2304.0	1444.8	26.6
70	171.8	400.0	2400.0	1444.8	27.7
81.5	179.8	320.0	1669.6	1661.6	19.3
83	182	88.0	3520.0	216.7	40.6

Hydrogen Verification Experiments (4 of 4)

VERIFICATION HYDROGEN EXPERIMENTS

RUN: verification 7: factor levels 3-1-1: 9/28/93

Rotameter	10.0				
Pressure	14.7	psia		SG	0.06944444
Flow (scfh)	48.7	H2		amb. T	84.5 F
mass	40.0			Q Value	60958.0 BTU/lb
Flow V =	0.01333681	cu.ft./s		AVG. EFF.	49.0
Flow m =	0.241604	lb/hr		STD.DEV.	6.2
Q supplied =	14,728	BTU/hr		LUMP EFF.	47.8

Time (min)	Temp (F)	Q(t)	Q(t)/t	Q(t)-Th.	Effic.(%)
0	81.8	0.0	0.0	0.0	0.0
3	92.2	416.0	8320.0	736.4	56.5
6	102	392.0	7840.0	736.4	53.2
9	112.2	408.0	8160.0	736.4	55.4
12	122.8	424.0	8480.0	736.4	57.6
15	132	368.0	7360.0	736.4	50.0
20	147.8	632.0	7584.0	1227.3	51.5
25	161.6	552.0	6624.0	1227.3	45.0
30	175.8	568.0	6816.0	1227.3	46.3
35	188.6	512.0	6144.0	1227.3	41.7
40	200.8	488.0	5856.0	1227.3	39.8
44.35	212	448.0	6179.3	1067.8	42.0